

Myriocin-induced adaptive laboratory evolution of an industrial strain of *Saccharomyces cerevisiae* reveals its potential to remodel lipid composition and heat tolerance

Journal:	<i>Microbial Biotechnology</i>
Manuscript ID	MICROBIO-2020-053-RA
Wiley - Manuscript type:	Research Article
Date Submitted by the Author:	04-Feb-2020
Complete List of Authors:	Randez-Gil, Francisca; Consejo Superior de Investigaciones Científicas, Department of Biotechnology, Instituto de Agroquímica y Tecnología de los Alimentos; Prieto, Jose Antonio; Instituto de Agroquímica y Tecnología de los Alimentos, Biotechnology Casas, Josefina; Consejo Superior de Investigaciones Científicas, Research Unit on BioActive Molecules (RUBAM), Instituto de Química Avanzada de Cataluña Estruch, Francisco; Universitat de València, Departament of Biochemistry and Molecular Biology
Keywords:	<i>Saccharomyces cerevisiae</i> , baker's yeast, cold, heat-stress, sphingolipid, elongase, myriocin

1
2
3
4
5
6
7
8
9
10
11
12
13
14
15
16
17
18
19
20
21
22
23
24
25
26
27
28
29
30
31
32
33
34
35
36
37
38
39
40
41
42
43
44
45
46
47
48
49
50
51
52
53
54
55
56
57
58
59
60

Myriocin-induced adaptive laboratory evolution of an industrial strain of *Saccharomyces cerevisiae* reveals its potential to remodel lipid composition and heat tolerance

Francisca Randez-Gil^{a,*}, Jose A. Prieto^a, Alejandro Rodríguez-Puchades^a, Josefina Casas^{b,c}, Vicente Sentandreu^d and Francisco Estruch^e

^a Department of Biotechnology, Instituto de Agroquímica y Tecnología de los Alimentos, Consejo Superior de Investigaciones Científicas, Avda. Agustín Escardino, 7. 46980-Paterna, Valencia, Spain

^b Research Unit on BioActive Molecules (RUBAM), Instituto de Química Avanzada de Cataluña, Consejo Superior de Investigaciones Científicas, Jordi Girona 18-26. 08034-Barcelona, Spain

^c CIBER-EHD, Instituto de Salud Carlos III, Monforte de Lemos 3-5. 28029-Madrid, Spain

^d Genomics Section, Central Service for Experimental Research (SCSIE), Universitat de València, Dr. Moliner 50, Burjassot 46100, Spain^e Departament of Biochemistry and Molecular Biology, Universitat de València, Dr. Moliner 50, Burjassot 46100, Spain

* For correspondence: E-mail: randez@iata.csic.es; Fax: +34 963636301; Tel: +34 963900022

Summary

The modification of lipid composition allows cells to adjust membrane biophysical properties in response to changes in environmental temperature. Here, we use adaptive laboratory evolution (ALE) in presence of myriocin, a sphingolipids (SLs) biosynthesis inhibitor, to remodel the lipid profile of an industrial yeast strain (LH) of *Saccharomyces cerevisiae*. The approach enabled to obtain a heterogeneous population (LHev) of myriocin-tolerant evolved clones characterized by its growth capacity at high temperature. Myriocin exposure also caused tolerance to soraphen A, an inhibitor of the acetyl-CoA carboxylase *Acc1*, the rate-limiting enzyme in fatty acid de novo production, supporting a change in lipid metabolism during ALE. In line with this, characterization of two randomly selected clones, LH03 and LH09, showed the presence of lipids with increased saturation degree and reduced acyl length. In addition, the clone LH03, which displays the greater improvement in fitness at 40°C, exhibited higher SLs content as compared with the parental strain. Analysis of the LH03 and LH09 genomes revealed a loss of chromosomes affecting to genes that have a role in fatty acid synthesis and elongation. The link between ploidy level and growth at high temperature was further supported by the analysis of a fully isogenic set of yeast strains with ploidy between 1N and 4N which showed that the loss of genome content provides heat-tolerance. Consistent with this, a thermotolerant evolved population (LH40°) generated from the parental LH strain by heat-driven ALE exhibited a reduction of the chromosome copy number. Thus, our results identify myriocin-driven evolution as a powerful approach to investigate the mechanisms of acquired thermotolerance and to generate improved strains.

Keywords: *Saccharomyces cerevisiae*; baker's yeast; heat-stress; sphingolipid; phospholipid; sphingoid bases; triacylglyceride; ploidy level

Abbreviations:

ALE, Adaptive laboratory evolution; Cer, Ceramides; CoA, Coenzyme A; DAG, Diacylglycerol; DhC, Dihydroceramide; DhS, Dihydrosphingosine; IPC, Inositol phosphorylceramide; LCBs, Long-chain bases; MIPC, Mannosylinositol phosphorylceramide; Myr, Myriocin; NLs, Neutral lipids; PA, Phosphatidate; PC, Phosphatidylcholine; PE, Phosphatidylethanolamine; PG, Phosphatidylglycerol; PhC, Phytoceramide; PhS, Phytosphingosine; PI, Phosphatidylinositol; PLs, Phospholipids; PS, Phosphatidylserine; SE, Steryl esters; SLs, Sphingolipids; SPT, Serine palmitoyltransferase; SorA, Soraphen A; TAG, Triacylglycerol; VLCFA, Very-long chain fatty acid;

Introduction

Commercial yeasts are mainly *S. cerevisiae* strains domesticated under artificial selection conditions. They are diploid, triploid, tetraploid, and polyploid, and some of them are aneuploids, which is the state characterized by having an abnormal number of certain chromosomes (Sicard and Legras, 2011; Duan *et al.*, 2018). Polyploidization events are frequently associated with the acquisition of broad phenotypic traits, such as robustness, large cell size, and high growth rate (Scott *et al.*, 2017), although it could also represent a way for yeast cells to develop phenotypic innovation and adaptation to the various stresses they have to confront in their industrial uses, such as baking, brewing, wine making, or bioethanol production (Fay and Benavides, 2005, Legras *et al.*, 2007; Randez-Gil *et al.*, 2013; Legras *et al.*, 2018). In addition, aneuploidy may induce genomic instability, as has been recently demonstrated (Sheltzer *et al.*, 2011; Zhu *et al.*, 2012), and thus could facilitate the development of genetic variants. However, this ploidy shift appears to have negative consequences in the behaviour of yeast cells under stress conditions (Randez-Gil *et al.*, 2013). Large-scale transitions in genome size from tetraploid or triploid to diploid as the predominant vegetative state of *S. cerevisiae* have been observed during long-term evolution experiments under stress conditions (Gerstein *et al.*, 2006; 2008; Aguilera *et al.*, 2010; Voordeckers *et al.*, 2015). Thus, the design of domesticated industrial yeasts by polyploidization may not favour the acquisition of stress tolerance phenotypes.

Thermotolerance in yeast is of major importance. Industrial heat-tolerant yeast strains are currently used for bioethanol production because the fermentations at high temperature ($\geq 40^{\circ}\text{C}$) facilitate the activity of saccharification enzymes and reduce production costs (Abdel-Banat *et al.*, 2010). On the other side, the ability of ferment at lower temperature than the optimal is a desired feature of wine and cider yeasts. Cold fermentations reduce the risk of undesirable contaminations during the production process and increase the aromatic complexity of these products (Pérez-Torrado *et al.*, 2018). Likewise, new species of baker's yeast strains with improved cryoresistance would be also very welcome for frozen dough applications (Randez-Gil *et al.*, 2013). Moreover, drying to obtain active dried yeast (ADY) or instant dried yeast (IDY) (Deák, 2003), impose extreme heat-stress conditions on baker's yeast cells that cause cellular damage, leakage of cell constituents, and loss of viability. Consequently, manipulation of growth protocols, thermal stress pre-adaptations and selection of individuals exposed

1
2
3 to extreme temperatures during the production processes, has been traditionally used to
4 provide certain thermotolerance. In the practice, the selection and development of cold-
5 and heat-tolerant yeast strains is still a challenge, and the clarification of the genomics
6 of thermal stress tolerance constitute an interesting and promising task.
7
8
9

10 Previous studies have revealed several mechanisms involved in thermal tolerance
11 acquisition, being likely lipid homeostasis the most important (Caspeta *et al.*, 2014; Liu
12 *et al.*, 2017). Lipids are essential components of eukaryotic membranes and the main
13 determinants of their functionality as cellular barriers. In yeast, a lower environmental
14 temperature brings about a change in membrane lipid composition, characterized by an
15 increased abundance of phospholipids (PLs) with shorter chain lengths and/or
16 unsaturated fatty acids (Rodríguez-Vargas *et al.*, 2007). On the contrary, membrane
17 fluidity increases in heat-stressed yeast cells, which appears to trigger lipid homeostasis
18 mechanisms to sustain membrane functionality. By using adaptive laboratory evolution
19 (ALE) to generate heat-stress tolerant evolved clones, Caspeta *et al.* (2014) identified
20 increased sterols accumulation as a mechanism to regulate membrane fluidity and allow
21 improved thermotolerance. Evidence also links the heat-shock response in *S. cerevisiae*
22 to the activation of sphingolipids (SLs) regulatory networks (Sun *et al.*, 2012), which
23 leads to the rapid and transient accumulation of long-chain bases (LCBs) and ceramides
24 (Cer) (Dickson *et al.*, 1997; Jenkins *et al.*, 1997), the precursors of complex SLs
25 (Megyeri *et al.*, 2016). Complex SLs with very-long chain fatty acids (VLCFAs) exhibit
26 a higher affinity for sterols, and together with them, promote the formation of a thicker,
27 more compact and less permeable plasma membrane than that provided by a lipid
28 matrix which contains high proportions of unsaturated PLs (Lester *et al.*, 2013).
29
30
31
32
33
34
35
36
37
38
39
40
41
42

43 Yeast adaptation to thermal stress may be also favoured by mutations in genes or
44 molecular pathways involved in membrane organization. Like other eukaryotic cell
45 plasma membranes, the *S. cerevisiae* membrane is asymmetric with an enrichment of
46 phosphatidylserine and phosphatidylethanolamine on the inner leaflet (Muthusamy *et al.*
47 *et al.*, 2009). This phospholipid asymmetry is established and maintained by lipid
48 translocases or flippases, encoded in yeast by five genes, *DRS2*, *NEO1*, *DNF1*, *DNF2*
49 and *DNF3* (López-Marqués *et al.*, 2011). Studies in our lab (García-Marqués *et al.*,
50 2016) and others (Hua *et al.*, 2002; Saito *et al.*, 2004) have identified phospholipid
51 asymmetry as an important aspect that influences cold tolerance by modifying the
52 composition and activity of plasma membrane-associated proteins. Interestingly,
53 flippase mutants also show resistance to myriocin, a well-known inhibitor of serine
54
55
56
57
58
59
60

1
2
3 palmitoyl transferase, SPT (Wadsworth *et al.*, 2013), the first enzyme in the *de novo*
4 SLs biosynthesis pathway (Megyeri *et al.*, 2016) that enters the cells via the action of
5 flippases (Khakhina *et al.*, 2015).
6
7

8 Here, we have induced genomic changes in an industrial yeast strain of *S. cerevisiae*
9 by ALE in the presence of myriocin. Our hypothesis was that myriocin-driven evolution
10 could be a suitable strategy to modify the lipid composition and/or asymmetry of the
11 plasma membrane, and as a result, the thermal adaptation of industrial strains. The
12 results presented in this work validate this strategy and add new knowledge on the
13 mechanisms that guide the yeast response to changes in environmental temperature. The
14
15
16
17
18
19
20
21

22 **Results and discussion**

23 *Adaptive evolution in the presence of myriocin*

24 We used a robust industrial baker's yeast strain named L'Hirondelle (LH) in order to
25 force by ALE changes in the lipid metabolism. For this, yeast was propagated by
26 successive batch refreshments maintained constantly in the presence of myriocin at
27 30°C during 50 generations (see Fig. 1A). In these experiments a chronic-medium dose
28 of 1.2 μM myriocin was used to lower but not completely inhibit SPT activity (Huang *et al.*,
29 2014; Fig. 1B). Moreover, a short-term experiment was chosen because deleterious
30 mutations, which could affect negatively important traits of industrial strains, such as
31 cell size, fitness or carbon-source utilization (Aguilera *et al.*, 2010; Çakar *et al.*, 2012;
32 Wenger *et al.*, 2011; Strucko *et al.*, 2018), have been reported to accumulate over time
33 (Tenailon *et al.*, 2016). In general, the rates of spontaneous mutation are higher for
34 neutral and deleterious mutations and lower for beneficial mutations (Barrick and
35 Lenski, 2013; Van den Bergh *et al.*, 2018). In this manner, we seek to generate evolved
36 clones containing stable compensatory mutations conferring increased SLs biosynthesis
37 (see Fig. 1B) or altered phospholipid asymmetry, but still maintaining key industrial
38 properties. We found that the doubling time decreased gradually over the course of the
39 experiment (data not shown), indicating that the original yeast population was capable
40 of adapting to optimize growth in the presence of the drug. As shown in Fig. 1C, the 50-
41 generations evolved population (LHev) grew in a solid myriocin-containing YPD
42 medium, while the parental strain did not. As expected, tolerance to myriocin was also
43 observed for ten individual adaptive clones isolated from the terminal population. In
44
45
46
47
48
49
50
51
52
53
54
55
56
57
58
59
60

1
2
3 addition, all of them showed a similar growth (Fig. 1C), suggesting that adaptation-
4 driving mutations were distributed across the population (Tenailon *et al.*, 2016).
5
6
7

8 *The evolved population shows increased tolerance to soraphen A*

9
10 We tested the growth of the experimental population and individual clones in the
11 presence of soraphen A (Fig. 1C), an inhibitor of acetyl CoA carboxylase, ACC (Gerth
12 *et al.*, 1994; Vahlensieck *et al.*, 1994; Gerth *et al.*, 2003; Hofbauer *et al.*, 2014). ACC
13 inhibitors lower malonyl-CoA content, interfere with fatty acid elongation and alter
14 cellular composition of lipid classes and sub-classes (Jump *et al.*, 2011; see also Fig.
15 1B). We reasoned that if myriocin-directed evolution caused global changes in lipid
16 metabolism, this would be reflected in a change of tolerance to soraphen A. On the
17 contrary, if selection had altered the myriocin uptake mechanisms, resistance to
18 soraphen A would remain unchanged. Myriocin and soraphen A differ in chemical
19 nature and it may be predicted they use different internalization mechanisms and do not
20 display drug synergy (Yilancioglu *et al.*, 2014). As it is shown, cells of either, the
21 terminal experimental population LHev or the individual clones (LH01-10), displayed
22 increased tolerance to soraphen A as compared with that of the original population LH
23 (Fig. 1C). Nevertheless, the improvement in drug tolerance differed among individuals
24 indicating that the evolution experiment generated phenotypic diversity.
25
26
27
28
29
30
31
32
33
34
35
36
37

38 *Myriocin-driven evolution alters yeast growth at different temperatures*

39
40 We asked whether the changes in myriocin tolerance observed in the evolved population
41 were relevant for the physiological response to thermal stress. As shown in Fig. 2,
42 growth at 30°C, the optimal temperature for *S. cerevisiae*, of the yeast population was
43 unaffected by the evolutionary experiment. On the contrary, the terminal population
44 exhibited increased growth at 40°C as compared with the parental, whereas a trade-off
45 in cell proliferation under cold conditions was observed (Fig. 2). Likewise, most of the
46 selected clones under study (LH01-LH10) exhibited increased fitness at 40°C (data not
47 shown) although again the phenotype differed quantitatively among individuals as it is
48 illustrated for two randomly selected clones, LH03 and LH09 (Fig. 2). Thus, the clone
49 LH09 exhibited only a slight growth advantage at 40°C, as compared with the parental
50 LH strain, while the LH03 clone grew much faster and had a similar behaviour to that of
51 the LHev population. Finally, these phenotypes correlated again with a loss in cold-
52
53
54
55
56
57
58
59
60

1
2
3 growth (Fig. 2). We conclude that myriocin-drive evolution improved yeasts ability to
4 adapt to increased temperature with no apparent trade-offs at the ancestral optimal
5 temperature of 30°C. The results also highlight how tolerance to high temperature is
6 associated with fitness impairments under cold-stressful conditions.
7
8
9

10 11 12 *SLs composition of evolved clones*

13
14 We analysed more in deep whether our evolutionary experiment forced a change in the
15 lipid metabolism of yeast cells. The SLs profile of the evolved clones LH03 and LH09
16 was analysed by LC-MS/MS and the results compared with those of the parental LH
17 strain. As shown in Fig. 3A, the evolved clone LH03 showed a higher content of SLs
18 than the parental LH strain, while the changes in LCBs or in the amount of SLs of the
19 clone LH09 were not statistically significant. We also observed a distinct behaviour
20 within the SLs sub-classes of the LH03 strain (Fig. 3B). Indeed, the relative abundance
21 of Cer-B, IPC-B and MIPC-B increased in cells of this strain, while that of the serie-C
22 members decreased (Fig. 3B). This was also evident in the major species of each sub-
23 class (Supplementary Tables S1-S3). The classical yeast SLs nomenclature establish five
24 sub-classes of Cer, IPC, MIPC and M(IP)₂C; A, B, B', C and D, according to their
25 hydroxylation degree (Megyeri *et al.*, 2016). In our analysis, species from the serie-B
26 and B', which contain both three OH groups, are indistinguishable, and those of the
27 serie-D cannot be determined. Molecules of the serie-C (four OH) are formed from
28 those of the serie-B by hydroxylation catalysed by the enzyme Scs7 (Haak *et al.*, 1997;
29 see Fig. 3C). Finally, we also observed a significant increase of C42-species of Cer and
30 C44-species of IPC and MIPC, and a parallel decrease of those of C46 in the LH03
31 strain (Fig. 3D). Since we used a mass spectrometry protocol without fragmentation, we
32 cannot distinguish between the contribution of the LCB or the acyl group to the total
33 chain length. Nevertheless, it is clear that the evolved clone LH03 forms SLs with
34 statistically shorter chain length.
35
36
37
38
39
40
41
42
43
44
45
46
47
48
49
50

51 52 *Myriocin-dependent regulation of neutral lipids and phospholipids*

53
54 Lipid metabolic pathways are highly interconnected in order to obtain a balanced
55 composition of classes and sub-classes of lipids. Accordingly, we examined the type
56 and amount of neutral lipids (NLs) and PLs in the evolved clones under study.
57 Compared with the parental strain, the mutant strains analysed did not show significant
58
59
60

1
2
3 changes in their absolute content of NLs and PLs (Supplementary Fig. S1). Neither their
4 relative abundance (mol%) of steryl esters (SE), diacylglycerol (DAG), triacylglycerol
5 (TGA), phosphatidate (PA), phosphatidylcholine (PC), phosphatidylethanolamine (PE),
6 phosphatidylglycerol (PG), phosphatidylinositol (PI) and phosphatidylserine (PS)
7 showed apparent variations (Fig. S1). However, the composition of molecular species
8 revealed noticeable changes (Supplementary Tables S4-S12), affecting mainly chain
9 length and insaturation degree. In general, PLs (Fig. 4 and Tables S7-S12) and NLs
10 (Tables S4-S6) species with shorter chain length and increasing saturation state became
11 more abundant in response to chronic myriocin exposure. Unlike the SLs data showed
12 above, similar results were observed for both evolved clones, LH09 and LH03, although
13 the changes were quantitatively more pronounced for LH03 cells. Such changes could
14 have a great impact in membrane properties, and thus, they could affect the adaptive
15 response to thermal stress and influence the phenotypic traits of the evolved population.
16 For example, increased SLs content and lower acyl desaturation could be expected to
17 rigidify the plasma membrane, and thus compensating for enhanced membrane fluidity
18 at high temperature. However, shorter acyl backbones have the opposite effect. Hence,
19 the attenuation of fatty acid elongation in the evolved clones could be mainly a
20 determinant not of heat tolerance but of increased resistance to myriocin toxicity.
21
22
23
24
25
26
27
28
29
30
31
32
33
34
35

36 *Phenotypic characterization of elo mutants*

37
38 The above results identified the fatty acid elongation as one of the lipid metabolic
39 processes altered in both LH03 and LH09 by the 50-generation myriocin exposure. The
40 products of three genes in *S. cerevisiae* have an important role in this process, *ELO1*,
41 *ELO2* and *ELO3*, which take place in the endoplasmic reticulum (Tehlivets *et al.*,
42 2007). The elongase Elo1 extends C12-C16 fatty acyl-CoAs to C16-C18 fatty acids
43 (Toke and Martin, 1996), while Elo2 elongates palmitoyl-CoA and stearoyl-CoA up to
44 C22 fatty acids, and Elo3 produces C20-C26 VLCFAs, which form part of Cer and
45 complex SLs (Megyeri *et al.*, 2016), from C18-CoA primers (Oh *et al.*, 1997; Rössler
46 *et al.*, 2003). Fig. 5A shows a schematic representation of the fatty acid elongation process
47 in yeast cells. Thus, changes in Elo1 activity may have effects in acyl constituents of all
48 lipid classes, SLs, NLs or PLs, while those in Elo2 and Elo3 could alter mainly the SLs
49 composition. According to this, we first examined the growth of the *elo1*, *elo2* and *elo3*
50 mutants of the laboratory wild-type strain BY4741 in liquid YPD medium containing or
51
52
53
54
55
56
57
58
59
60

1
2
3 lacking myriocin and soraphen A. As shown in Fig. 5B, knock-out of *ELO2* or *ELO3*
4 caused a clear defect in the growth of wild-type cells in YPD control medium at 30°C,
5 while no significant effect could be detected by the absence of Elo1. Despite of this,
6 cells devoid of Elo2 activity grew much better than the wild-type in the presence of
7 myriocin (Fig. 5B), a result previously reported by Olson *et al.* (2015) in a different
8 yeast background. Furthermore, the lack of Elo3 provided a statistically significant
9 growth advantage, but the effect was scarce, while no effect could be detected in *elo1*
10 mutant cells (Fig. 5B). On the other hand, cells lacking the elongase activity provided
11 by Elo2 or Elo3 were unable to grow in soraphen A-containing medium, suggesting that
12 the synthesis of Cer and/or complex SLs could be critical when cells are exposed to
13 Acc1 inhibitors. On the contrary, mutation of *ELO1* rendered yeast cells more tolerant
14 to soraphen A (Fig. 5B).

15
16 We then analysed the growth of the mutants at 40°C (Supplementary Fig. S2).
17 Again, *elo2* and *elo3* strains showed, as compared with the wild-type, a growth defect
18 similar to that observed at the optimal 30°C temperature (Fig. 5B; YPD). Neither the
19 loss of Elo1 caused an apparent advantage under high temperature conditions (Fig. S2).
20 Finally, we checked the phenotypes of cells lacking the hydroxylase Scs7. We were
21 unable to observe increased growth in the presence of myriocin or aureobasidin A (data
22 not shown), or in response to thermal stress (Fig. S2). Taken together, these results
23 suggest that a reduced elongase activity might be a determinant of the myriocin- and
24 soraphen A-tolerance phenotype exhibited by the industrial evolved clones. The
25 relationship between this activity and heat tolerance is however unclear.

26 27 *Adaptive laboratory evolution causes aneuploidy and loss of ELO-genes* 28 29 *copy number*

30
31 The emergence of aneuploidy, including whole-chromosome loss, in response to
32 different environmental and stressful conditions has been widely observed in a wide
33 range of organisms (Ben-David and Amon, 2020), including *S. cerevisiae* (Gerstein *et al.*,
34 2006; 2008; Aguilera *et al.*, 2010; Voordeckers *et al.*, 2015; Pavelka *et al.*, 2010;
35 Selmecki *et al.*, 2015). Accordingly, we analysed the genomes of the two evolved
36 clones isolated from the industrial LH strain. First, we examined the DNA content by
37 flow cytometry (Fig. S3). As we expected, the ploidy of the parental and the evolved
38 populations was higher than that of the laboratory strains used as control, BY4741 (1N,
39
40
41
42
43
44
45
46
47
48
49
50
51
52
53
54
55
56
57
58
59
60

haploid) and BY4743 (2N, diploid). Interestingly, the DNA content per cell decreased in both evolved strains after 50-generations of myriocin exposure. Thus, the estimated average chromosome number for the parental strain (LH) was 4.1, whereas for LH03 was 3.0 and 3.6 for LH09. This reduction was confirmed by the chromosome-copy number predictions from the sequencing data (Table 1). Indeed, the likelihood ploidy for the sixteen chromosomes of the parental strain was tetraploid, while there was a reduction in the number of copies in nine of the chromosomes of strain LH03 and in three of the chromosomes of strain LH09.

Then, we check whether the ploidy reduction observed in the evolved strains altered the lipid-gene doses, in particular of those whose activity may influence the acyl chain length (Table 1). Indeed, we found that LH03 cells lost a copy of the chromosomes III, X and XII, where the genes *ELO2*, *ELO1* and *ELO3* are located, respectively (Table 1). In addition, the myriocin-evolved approach resulted in a reduction of the copy-number of genes involved in fatty acid activation (*FAA2* and *FAA4*) and synthesis (*FAS2*), which could contribute to the changes observed in the acyl chain length of NLs and PLs of both, LH03 and LH09 (Fig. 4 and Tables S4-S12). Finally, we also noted that cells of the clone LH03, but not those of the clone LH09, lost a copy of the hydroxylase-encoding gene *SCS7* (Table 1; chromosome XIII), which could explain the decrease in the relative abundance of SLs species of the serie-C found in the former (Fig. 3B).

Point mutation analysis

The whole-genome sequencing data were further analysed in search of single-nucleotide polymorphisms (SNPs). The identification of point mutations occurred during evolution proved to be difficult because the elevated ploidy of the strains and the chromosome copy number variation observed. For these reasons, the SNP calling was settled on an approach that required >15% base-call supporting a SNP in the evolved genomes and <5% base-call supporting the same base in the parental genome data and genotype quality above 20. Applying this approach we detected 78 single point mutations found only in the evolved LH03 strain (Table S13) whereas 10 SNPs were only found in the evolved LH09 strain (Table S14) and 28 were found in both evolved strains (Table S15). The most striking result was observed in the SNPs detected in the LH03 strain. Most of the polymorphisms found in coding regions were located in ribosomal protein coding genes (45 out of a total of 60). Even more striking is that all the changes

1
2
3 identified give synonymous variants. A detailed analysis of the amino acids affected by
4 these changes reveals that they are mostly non-polar (31 of 45) and that the changes
5 give rise to triplets with a lower codon usage value (26 SNPs increase this value while
6 15 reduce it). These changes could lead to the attenuation of the levels of ribosomal
7 proteins translation, which in turn might improve the fitness of the aneuploid evolved
8 clones by reducing proteotoxic stress. Evidence of a link between protein synthesis rate
9 and several phenotypes shared by all aneuploidy human cells has been reported (Torres
10 *et al.*, 2007; Oromendia *et al.*, 2012). On the other hand, SLs are synthesized from
11 serine and palmitoyl-CoA (Megyeri *et al.*, 2016), and consequently reduced protein
12 translation could increase the availability of this amino acid and the levels of SLs as it
13 was observed in the LH03 strain (Fig. 3A).

14
15 In relation to the SNPs identified exclusively in strain LH09 or that are common in
16 both evolved strains, we find remarkable the N370D polymorphism (present in both
17 strains) that affects the *CST26* gene, encoding an acyltransferase enzyme responsible for
18 the introduction of saturated very long chain fatty acids into phosphatidylinositol (Le
19 Guédard *et al.*, 2009). Interestingly, this gene was initially identified in a search for
20 genes that affect chromosome stability (CST) when overexpressed in *S. cerevisiae*
21 (Ouspenski *et al.*, 1999). Hence, the changes identified in this gene may be associated to
22 the genomic instability and increased chromosome loss displayed by the evolved clones.

23 24 *Loss of ploidy level drives adaptation to heat-stress*

25
26 To gain insight into how chromosome loss affects the phenotypic characteristics of the
27 LHev evolved population, we first compared the growth at high temperature of an
28 isogenic series of diploid (2N), triploid (3N) and tetraploid (4N) yeasts generated from
29 the haploid (1N) laboratory strain BY4741 (Storchová *et al.*, 2006). As it is shown in
30 Fig. 6A, loss of chromosome-copy number provided a fitness advantage to yeast cells
31 grown at 40°C in either YPD or minimal SCD medium, while no effect was observed at
32 the optimal 30°C temperature. Quite remarkably, the increased growth was correlated
33 with the loss of ploidy level ranking from 4N to 1N (Fig. 6A). Next we compared the
34 growth under different environmental conditions, such as H₂O₂-mediated oxidative
35 stress, hyperosmotic NaCl or presence of tunicamycin, which induces endoplasmic
36 reticulum stress. Under all these conditions, the analysed strains grew similarly (Fig.
37 S4). Neither the ploidy level had a noticeable effect on the growth of yeast cells in SCD
38
39
40
41
42
43
44
45
46
47
48
49
50
51
52
53
54
55
56
57
58
59
60

1
2
3 culture medium containing myriocin, aureobasidin or soraphen A (Fig. S4). Our results
4 indicate a strong relevance of ploidy level in the context of thermotolerance, an effect
5 that could be related to proteotoxicity. It has been reported that yeast strains harbouring
6 an additional copy of a single yeast chromosome, called disomes, display a higher load
7 of endogenous protein aggregates and exhibit increased sensitivity to high temperature
8 (Oromendia *et al.*, 2012). In addition, proteotoxicity is also a hallmark of heat-stress
9 (Joutsen *et al.*, 2020). However, the fact that polyploidy did not alter growth in the
10 presence of tunicamycin (a condition that also requires the assistance of the cell's
11 protein quality-control pathways; Fig. S4) is indicative of the complex relationship
12 between thermal stress and ploidy.
13
14
15
16
17
18
19

20 Finally, we wonder whether adaptation to high temperature in the industrial strain
21 selects cells with decreased ploidy level. Like the myriocin-driven experiment, cells of
22 the parental yeast LH were propagated by successive batch refreshments maintained
23 constantly at 40°C during 50 generations and the DNA content of the evolved
24 population (LH40°) was examined by flow cytometry. As expected, heat exposure
25 promoted a loss of chromosome-copy number in the heat-exposed terminal population
26 (2.9N). Similar decreases were also observed for isolated clones from LH40° (data not
27 shown).
28
29
30
31
32
33
34
35

36 *Heat- and myriocin-evolved populations display common and distinct* 37 *phenotypes*

38 We wonder if our initial choice of myriocin as evolutionary condition to select, among
39 others, thermotolerant strains was appropriate in terms of biotechnological suitability. In
40 this context, the best phenotype is not always necessarily the one with the highest
41 fitness, but the one that shows increased performance and the least trade-offs in other
42 environmental conditions (Dragosits and Mattanovich, 2013). Thus, we compared the
43 phenotypic profile of heat- and myriocin-evolved industrial yeast cells. As expected, the
44 heat-evolved population exhibited higher fitness at 40°C than the LHev, and this late
45 grew much faster than the LH40° in the presence of myriocin (Fig. 6B). Furthermore,
46 both evolved populations exhibited increased tolerance to H₂O₂ (data not shown) or to
47 either tunicamycin or DTT (Fig. 6B), indicating likely cross-protection (Dragosits and
48 Mattanovich, 2013). More importantly, the cells that were evolved under heat show an
49 evident growth trade-off at the optimal growth temperature for yeast (Fig. 6B; 30°C).
50
51
52
53
54
55
56
57
58
59
60

1
2
3 Based on these data, the myriocin approach appears as an interesting strategy to isolate
4 industrially-relevant yeast strains.
5
6
7

8 **Concluding remarks**

9
10
11 Our study points out the importance of downregulating the fatty acid elongation as a
12 mechanism to face with the SLs-biosynthesis inhibition. The key players of this
13 regulation were the reticulum endoplasmic elongases Elo1, Elo2 and Elo3, although
14 impaired cytosolic fatty acid synthase activity may be on the basis of the shorter fatty
15 acids exhibited by NLs and PLs in the clone LH09. The activity of all these enzymes
16 involves the condensation/decarboxylation of acyl-CoA with Acc1-derived malonyl-
17 CoA (Tehlivets *et al.*, 2007). Thus, decreased elongase activity reduces the demand of
18 malonyl-CoA and increases the availability of palmitoyl-CoA, the precursor together
19 with serine of LCBs, alleviating likely the myriocin-instigated inhibition of SPT.
20 Consistent with this mechanism, the evolved clones showed increased resistance to
21 soraphen A, the Acc1 inhibitor, and displayed lower acyl desaturation degree. This
22 suggests the changes in saturation were likely addressed to provide an additional supply
23 of palmitoyl-CoA. Altogether, the findings underline the cross-talk between lipid
24 metabolic pathways, and the close interaction of fatty acid elongation and desaturation
25 with SLs metabolism.
26
27

28
29
30
31
32
33
34
35
36
37 Biochemical characterization of the evolved clones revealed differences that could
38 explain their phenotypic variation. Our results suggest that α -hydroxylation of Cer, IPC
39 and MIPC, in combination with the higher content of SLs, could play a role in the
40 acquired thermotolerance mechanism observed in the LH03 clone. It is well known that
41 heat-shock increases the yeast SLs content, contributing, together with sterols, to reduce
42 membrane fluidity at high temperature. The rationale to replace SLs of the serie-C by
43 those of the serie-B in that clone is less obvious, although it may be related with toxicity
44 differences between Cer sub-classes and species. It has been suggested that PhS-based
45 Cer are more toxic than DhS-based ones, while the acyl α -hydroxylation level seems to
46 reduce the toxicity of these compounds (Tani and Kuge, 2012). Hence, the change in the
47 profile of Cer could help to reduce the toxicity produced by elevated Cer levels.
48 Nevertheless, these changes could also play a role in heat-signalling or mediate the
49 regulation of structural properties of the plasma membrane at high temperature. More
50 work is required to clarify the physiological significance of these changes.
51
52
53
54
55
56
57
58
59
60

1
2
3 The myriocin-driven ALE approach selected evolved clones with a specific and
4 complex aneuploidy pattern. It has been proposed that aneuploidy generates
5 stoichiometric imbalance of protein complexes leading to proteotoxicity and reduced
6 fitness under non-stress conditions (Pavelka *et al.*, 2010; Chen *et al.*, 2019). However,
7 the evolved clones selected do not show major growth impairment at the ancestral
8 optimal growth temperature (Fig. 2; 30°C). In addition, the loss of chromosome copy
9 number provided a proliferative advantage to myriocin- and heat-exposed cells. SLs
10 levels are tightly linked to serine availability, which it is favoured by decreasing the
11 number of encoding genes (Torres, 2015; Hwang *et al.*, 2017), but more importantly,
12 decreasing ploidy level provided additional mechanisms of cell protection at high
13 temperature, that were confirmed by analysis of isogenic strains of BY4741 and heat-
14 driven evolved yeast populations. Whether this general effect is mediated by decreasing
15 proteotoxicity needs to be investigated.

16
17 Taken together, our evolutionary experiment demonstrates that is possible to obtain
18 phenotypic variation and growth advantages under industrially-relevant conditions that
19 do not inevitably result in important fitness drawbacks in the optimal environment.
20 Hence, the isolated clones in our study are of great value to gain insights about the
21 mechanisms of yeast adaptation and the seed of more robust stress-resistant strains.
22
23
24
25
26
27
28
29
30
31
32
33
34
35
36
37
38
39
40
41
42
43
44
45
46
47
48
49
50
51
52
53
54
55
56
57
58
59
60

Experimental procedures

Yeast strains and cultivation conditions

The *S. cerevisiae* strain L'Hirondelle (LH), a commercial baker's yeast produced by the Lesaffre Group (Lille, France) was used in the evolutionary experiments reported in this study. The laboratory *S. cerevisiae* strains BY4743 (diploid, 2N), BY4741 (haploid, 1N), BY4741-mutants *elo1*, *elo2*, *elo3* and *scs7*, all of them from the Euroscarf yeast collection (Oberursel, Germany), as well as a serie of BY4741-derived isogenic strains differing in ploidy level (2N, 3N and 4N; Storchová *et al.*, 2006) were also used. Cells were regularly maintained on solid YPD (20 g l⁻¹ agar, 20 g l⁻¹ peptone, 20 g l⁻¹ glucose and 10 g l⁻¹ yeast extract) or SCD (20 g l⁻¹ agar, 5 g l⁻¹ ammonium sulphate, 20 g l⁻¹ glucose, and 1.7 g l⁻¹ yeast extract without amino acids and ammonium sulphate) supplemented with the appropriate amino acid drop-out mixture (Formedium, England).

For plate phenotype experiments, cells were grown to the mid-exponential phase at 30°C (OD₆₀₀ ~ 0.5). Then, 10-fold serial dilutions were prepared and 3 µl aliquots of three dilutions (10⁻¹–10⁻³) were applied over the agar-gelled plates. Colony growth was inspected after 2-4 days of incubation at 12, 30 or 40°C. In some experiments, the growth under stressful conditions was followed in liquid medium. In this case, 30°C-grown saturated YPD-cultures were diluted in the appropriate medium at initial OD₆₀₀ ~ 0.025-0.05. Stock solutions of 1.0 mg/ml (methanol) soraphen A (a gift from R. Jansen) and 2 mM myriocin (ethanol:DMSO; 80:20, v:v) were prepared, sampled in small volumes and stored at -20°C until use. For each experiment, a fresh sample was thawed and diluted at the indicated concentration.

Laboratory adaptive evolution

Evolution experiments were conducted using batch culture techniques in a similar manner than that described by Aguilera *et al.* (2010). Fifty millilitres of medium YPD containing 1.2 µM myriocin (final concentration), was inoculated at OD₆₀₀ ~ 0.05 and cultured in 250 ml Erlenmeyer flasks at 30°C and 200 rpm. The culture was refreshed daily and cultivated in the same way until a minimum of ~ 50 generations was attained. Heat-driven ALE was conducted similarly except that cells were grown at 40°C in the absence of myriocin. As each transfer allowed ~ 6.64 mitotic divisions, a total of ~ 8 transfers were carried out. Samples from the evolved populations were taken, maintained as frozen (-80°C) glycerol stocks and then rescued in YPD agar plates at

1
2
3 30°C for 24 h before further analysis. These conditions preserved the characteristics of
4 the evolved population and ensured that yeast cells were growing under the same
5 conditions.
6
7

8 For the selection of adaptive clones within the myriocin-driven 50-generation
9 experimental population (LHev), a diluted sample was cultivated in solid YPD
10 containing 2.0 µM myriocin. Then, 10 cells that formed the biggest colonies, LH01-
11 LH10, were randomly selected, and preserved at -80°C for further characterisation.
12 Individual clones from the terminal heat-evolved population (LH40°) were also isolated
13 and preserved under the same conditions.
14
15
16
17
18
19

20 *SLs extraction and mass spectrometry analysis*

21 YPD-grown cells of the parental LH strain and the myriocin-evolved clones LH03 and
22 LH09 (OD₆₀₀ ~ 1.0) were collected by centrifugation (3,000 x g, 2 min, 4°C), washed
23 twice with ultrapure water (MilliQ RO 10 Plus; Millipore, Bedford, MA) and kept at -
24 80°C until the extraction was carried out. Then, the cell pellet was suspended in 300 µl
25 of ultrapure water, glass beads (1.0 g; acid washed, 0.4-mm diameter) were added, and
26 the mixture was vortexed 5 times for 1 min each time. Finally, the homogeneous broken
27 cell suspension was recovered, diluted with ultrapure water (~ 20 OD₆₀₀ units/ml), and
28 subjected to SLs analysis.
29
30
31
32
33
34
35

36 Sphingolipids were extracted according to a previous study (Barbacini *et al.*, 2019),
37 with minor modifications. Methanol (1 ml) and chloroform (0.5 ml) were added to 0.5
38 ml of the cell suspension, fortified with internal standards [200 pmol: sphinganine
39 (d17:0), sphinganine-1-phosphate (d17:0), and C12 Ceramide (d18:1/12:0)], vortexed,
40 and incubated at 48°C overnight. Then, KOH in methanol (1 M, 75 µL) was added and
41 incubated for 2 hr at 37°C. Finally, acetic acid (1 M, 75 µL) was added and samples
42 were evaporated and stored at -80°C. Methanol (80 µL) was added to the samples,
43 vortexed, centrifuged at 9,400 x g for 5 min and transferred into UPLC vials for their
44 analyses.
45
46
47
48
49
50
51

52 Cer, IPC and MIPC analysis was performed using an Acquity ultra-high
53 performance liquid chromatography (UHPLC) system (Waters) connected to a Time of
54 Flight (LCT Premier XE) detector. Full scan spectra from 50 to 1800 Da were acquired,
55 and individual spectra were summed to produce data points each of 0.2 sec. Mass
56 accuracy at a resolving power of 10,000 and reproducibility were maintained by using
57
58
59
60

1
2
3 an independent reference spray via the LockSpray interference. Lipid extracts were
4 injected onto an Acquity UHPLC BEH C8 column (1.7 μm particle size, 100 mm x 2.1
5 mm, Waters) at a flow rate of 0.3 mL/min and column temperature of 30 $^{\circ}\text{C}$. The mobile
6 phases were methanol with 2 mM ammonium formate and 0.2 % formic acid (A)/water
7 with 2 mM ammonium formate and 0.2 % formic acid (B). A linear gradient was
8 programmed. The gradient starts with 80% A and increases to 90% A in 3 min. After 3
9 min at 90% A the gradient increases to 99% A in 9 min and continues at 99% A for 3
10 min. During the following 2 min the column is readjusted to the initial conditions and
11 equilibrated for further 2 min. Phytosphingosine and phytosphingosine-1-phosphate
12 were analysed using an Acquity ultra-high performance liquid chromatography
13 (UHPLC) system (Waters) connected to a triple quadrupole (Xevo-TQ-S) detector. The
14 following transitions were used: 288.3>252.3 (C17 dihydrosphingosines), 302.3>284.4
15 (dihydrosphingosines), 318.3>282.4 (phytosphingosines), 382.4>284.4
16 (dihydrosphingosines-1-P), 398.4>282.4 (phytosphingosines-1-P). The same column,
17 mobile phases and gradient were used. The levels of the different lipid classes and
18 species in each sample were normalized as pmol eq/OD₆₀₀. All the data were calculated
19 from three biological replicates (\pm SD).
20
21
22
23
24
25
26
27
28
29
30
31
32
33

34 *NLs and PLs analysis*

35
36 Cell samples were processed as described above for SLs extraction and subjected to
37 basic lipidomic analysis. This was carried out by the lipidomic service of Lipotype
38 (Lipotype GmbH, Dresden, Germany), which use a high throughput mass-spectrometry-
39 based shotgun lipidomics platform. Lipids were extracted using chloroform and
40 methanol (Klose *et al.*, 2012). Samples were spiked with lipid-class specific internal
41 standards prior to extraction. After drying and resuspending in MS acquisition mixture,
42 lipid extracts were subjected to mass spectrometric analysis. Mass spectra were acquired
43 on a hybrid quadrupole/Orbitrap mass spectrometer equipped with an automated nano
44 flow electrospray ion source in both positive and negative ion mode. Lipid identification
45 using LipotypeXplorer (Herzog *et al.*, 2011) was performed on unprocessed (*.raw
46 format) mass spectra. For MS-only mode, lipid identification was based on the
47 molecular masses of the intact molecules. MSMS mode included the collision induced
48 fragmentation of lipid molecules and lipid identification was based on both the intact
49 masses and the masses of the fragments. Prior to normalization and further statistical
50
51
52
53
54
55
56
57
58
59
60

1
2
3 analysis, lipid identifications were filtered according to mass accuracy, occupation
4 threshold, noise and background. Lists of identified lipids and their intensities were
5 stored in a database optimized for the particular structure inherent to lipidomic datasets.
6 Intensity of lipid class-specific internal standards was used for lipid quantification. The
7 amounts of individual lipid molecules (species) of a given lipid class were normalized
8 as the mol%. Likewise, the quantities of the lipid species containing the same number of
9 double bonds or the same number of carbon atoms in the hydrocarbon moiety are
10 summed and these values are normalized to the total amount of the given lipid class.
11 Additional details concerning sample handling and processing, reagents, equipment,
12 procedures and data visualization tools can be found at <https://www.lipotype.com/>. Data
13 represent the mean value (\pm SD) of three independent biological replicates.
14
15
16
17
18
19
20
21
22
23

24 *Genome size*

25
26 Flow cytometric analysis was used to estimate the approximate genome size of the
27 industrial yeast strains. Cells were grown in liquid YPD to exponential phase, harvested,
28 washed and fixed in 70% ethanol at 4°C for 5 min. Then, cells were collected by
29 centrifugation and resuspended in 10 mM PBS buffer (pH = 7.2), containing 400 μ l of
30 RNase (10 mg ml⁻¹). After incubation at 37°C for 30 min, the cells were harvested by
31 centrifugation and resuspended in 1 ml of the same buffer containing 2.5 mg l⁻¹ of
32 propidium iodine. Samples were analysed using a flow cytometer FAC Scan analyser
33 (Becton Dickinson, USA). Ploidy determinations were done by comparing with the
34 laboratory strains BY4741 (1N) and BY4743 (2N).
35
36
37
38
39
40
41
42

43 *Sequencing and bioinformatics analysis*

44
45 Whole-genome sequencing and bioinformatics analysis were performed at the
46 Genomics service of the Valencia University (Valencia, Spain). Briefly, Illumina
47 sequencing libraries from LH, LH03 and LH09 strains were constructed using the
48 Truseq nano DNA library preparation kit (Illumina Inc., San Diego, CA). The number
49 of raw pair-end 301 bp reads collected were 6,341,808 (LH), 2,594,029 (LH03) and
50 7,264,515 (LH09). Raw reads were quality trimming and filtering using AfterQC (Chen
51 *et al.*, 2017), with filter of minimum phred-quality score 15 and minimum read size as
52 50. Raw and processed reads quality control was made with FastQC v0.11.8
53 (<http://www.bioinformatics.babraham.ac.uk>) and AfterQC tools. Resulting reads,
54
55
56
57
58
59
60

1
2
3 5,788,893 (LH), 2,413,082 (LH03) and 6,788,094 (LH09) were aligned to the *S.*
4 *cerevisiae* R64-1-1 reference strain using the bowtie2 mapping tool (Langmead and
5 Salzberg, 2012). Samtools 1.19 and Picard 2.18 (Li *et al.*, 2009) were used for mapping
6 post-processing and remove duplicates. Only proper paired reads with a mapping
7 quality score above 30 were retained from the alignment. Indel realignment and depth of
8 coverage calculation was performed with GATK-3.6.
9

10
11
12
13 Alignment data files were quality check with Qualimap v2.2.1 (García-Alcalde *et*
14 *al.*, 2012; Okonechnikov *et al.*, 2016). Percentage of reference bases covered above 4
15 reads were 93,2 % (LH), 93,1 % (LH03) and 93,2 % (LH09) with an average read-depth
16 of 171,75 (LH), 85,24 (LH03) and 228,76 (LH09). For SNP-calling (SNPs and indels
17 detection) and filtering we use VarScan (v2.3.9; `-min-avg-qual 20 -min-var-frequeation`
18 `0.05 -min-coverage 30 -min-reads2 5 -min-freq-for-hom 0.95 --p-value 0.05`).
19 MiModD 0.1.9 tool (<http://doi.org/10.5281/zenodo.2582000>) was used for variant post-
20 processing, including genotype filtering and annotation with SnpEff v4.3t (Cingolani *et*
21 *al.*, 2012) settled on approach that required >10% base-call supporting a SNP in the
22 evolved genomes and <2% base-call supporting the same base in the parental genome
23 data and genotype quality above 20. To detect chromosome copy-number changes we
24 use the nQuire tool (Weiß *et al.*, 2018) with mapping quality and minimum coverage
25 filters set to 10 and applying lrdmodel to assess ploidy level.
26
27
28
29
30
31
32
33
34
35
36
37

38 *Statistical analysis*

39 Sample averages were compared using a Student's *t*-test with the Excel software
40 (Microsoft). $p < 0.01$ (**) and $p < 0.05$ (*,#) were considered statistically significant.
41
42
43
44
45
46

47 **Acknowledgments**

48 We thank R. Jansen (Helmholtz Centre for Infection Research, Braunschweig,
49 Germany) for providing us with a sample of soraphen A. We also thank Isabel E.
50 Sánchez-Adriá and Gemma Sanmartín Peris for their help in preparing samples and
51 conducting experiments. We also acknowledge the technical assistance of Alexandre
52 García with SLs analysis. This research has been supported by the Comisión
53 Interministerial de Ciencia y Tecnología Project (BIO2015-71059-R) from the Spanish
54 Ministry of Science, Innovation and Universities (MICINN/FEDER), and the i-LINK
55 program (i-LINK1109) from the Spanish National Research Council (CSIC).
56
57
58
59
60

1
2
3
4
5 **Conflict of interest**
6

7 The authors declare they have no conflict of interest.
8
9
10
11
12
13
14
15
16
17
18
19
20
21
22
23
24
25
26
27
28
29
30
31
32
33
34
35
36
37
38
39
40
41
42
43
44
45
46
47
48
49
50
51
52
53
54
55
56
57
58
59
60

For Review Only

References

- Abdel-Banat, B.M., Hoshida, H., Ano, A., Nonklang, S., Akada, R. (2010) High-temperature fermentation: how can processes for ethanol production at high temperatures become superior to the traditional process using mesophilic yeast? *Appl Microbiol Biotechnol* **85**: 861-867.
- Aguilera, J., Andreu, P., Randez-Gil, F., Prieto, J.A. (2010) Adaptive evolution of baker's yeast in a dough-like environment enhances freeze and salinity tolerance. *Microb Biotechnol* **3**: 210-221.
- Barbacini, P., Casas, J., Torretta, E., Capitanio, D., Maccallini, G., Hirschler, V. *et al.* (2019) Regulation of Serum Sphingolipids in Andean Children Born and Living at High Altitude (3775 m). *Int J Mol Sci* **20**: E2835.
- Barrick, J.E., Lenski, R.E. (2013) Genome dynamics during experimental evolution. *Nat Rev Genet* **14**: 827-839.
- Ben-David, U., Amon, A. (2020) Context is everything: aneuploidy in cancer. *Nat Rev Genet* **21**: 44-62.
- Çakar, Z.P., Turanlı-Yıldız, B., Alkim, C., Yilmaz, U. (2012) Evolutionary engineering of *Saccharomyces cerevisiae* for improved industrially important properties. *FEMS Yeast Res.* **12**: 171-182.
- Caspeta, L., Chen, Y., Ghiaci, P., Feizi, A., Buskov, S., Hallström, B.M. *et al.* (2014) Biofuels. Altered sterol composition renders yeast thermotolerant. *Science* **346**: 75-78.
- Cingolani, P., Platts, A., Wang, le L., Coon, M., Nguyen, T., Wang, L. *et al.* (2012) A program for annotating and predicting the effects of single nucleotide polymorphisms, SnpEff: SNPs in the genome of *Drosophila melanogaster* strain w1118; iso-2; iso-3. *Fly (Austin)* **6**: 80-92.
- Chen, S., Huang, T., Zhou, Y., Han, Y., Xu, M., Gu, J. (2017) AfterQC: automatic filtering, trimming, error removing and quality control for fastq data. *BMC Bioinformatics* **18**(Suppl 3), 80.
- Chen, Y., Chen, S., Li, K., Zhang, Y., Huang, X., Li, T. *et al.* (2019) Overdosage of Balanced Protein Complexes Reduces Proliferation Rate in Aneuploid Cells. *Cell Syst* **9**: 129, e5.
- Deák, T., 2003. Yeasts. In: Encyclopedia of Food Sciences and Nutrition, ed. B Caballero, P Finglas, L Trugo, pp. 6233-39. London: Academic. 2nd ed.
- Dickson, R.C., Nagiec, E.E., Skrzypek, M., Tillman, P., Wells, G.B., Lester, R.L. (1997) Sphingolipids are potential heat stress signals in *Saccharomyces*. *J Biol Chem* **272**: 30196-30200.
- Dragosits, M., Mattanovich, D. (2013) Adaptive laboratory evolution -- principles and applications for biotechnology. *Microb Cell Fact* **12**: 64.
- Duan, S.F., Han, P.J., Wang, Q.M., Liu, W.Q., Shi, J.Y., Li, K. *et al.* (2018) The origin and adaptive evolution of domesticated populations of yeast from Far East Asia. *Nat Commun* **9**: 2690.
- Fay, J.C., Benavides, J.A. (2005) Evidence for domesticated and wild populations of *Saccharomyces cerevisiae*. *PLoS Genet* **1**: 66-71.
- García-Alcalde, F., Okonechnikov, K., Carbonell, J., Cruz, L.M., Götz, S., Tarazona, S. *et al.* (2012) Qualimap: evaluating next-generation sequencing alignment data. *Bioinformatics* **28**: 2678-2679.
- García-Marqués, S., Randez-Gil, F., Dupont, S., Garre, E., Prieto, J.A. (2016) Sng1 associates with Nce102 to regulate the yeast Pkh-Ypk signalling module in response to sphingolipid status. *Biochim Biophys Acta* **1863**: 1319-1333.

- 1
2
3 Gerstein, A.C., Chun, H.J., Grant, A., Otto, S.P. (2006) Genomic convergence toward
4 diploidy in *Saccharomyces cerevisiae*. *PLoS Genet* **2**: e145.
- 5 Gerstein, A.C., McBride, R.M., Otto, S.P. (2008) Ploidy reduction in *Saccharomyces*
6 *cerevisiae*. *Biol Lett* **4**: 91-94.
- 7
8 Gerth, K., Bedorf, N., Irschik, H., Höfle, G., Reichenbach, H. (1994) The soraphens: a
9 family of novel antifungal compounds from *Sorangium cellulosum* (Myxobacteria).
10 I. Soraphen A1 alpha: fermentation, isolation, biological properties. *J Antibiot*
11 (Tokyo) **47**: 23-31.
- 12 Gerth, K., Pradella, S., Perlova, O., Beyer, S., Müller, R. (2003) Myxobacteria:
13 proficient producers of novel natural products with various biological activities--past
14 and future biotechnological aspects with the focus on the genus *Sorangium*. *J*
15 *Biotechnol* **106**: 233-253.
- 16
17 Haak, D., Gable, K., Beeler, T., Dunn, T. (1997) Hydroxylation of *Saccharomyces*
18 *cerevisiae* ceramides requires Sur2p and Scs7p. *J Biol Chem* **272**: 29704-29710.
- 19 Henry, S.A., Kohlwein, S.D., Carman, G.M. (2012) Metabolism and regulation of
20 glycerolipids in the yeast *Saccharomyces cerevisiae*. *Genetics* **190**: 317-349.
- 21 Herzog, R., Schwudke, D., Schuhmann, K., Sampaio, J.L., Bornstein, S.R., Schroeder,
22 M. *et al.* (2011) A novel informatics concept for high-throughput shotgun lipidomics
23 based on the molecular fragmentation query language. *Genome Biol* **12**: R8.
- 24 Hofbauer, H.F., Schopf, F.H., Schleifer, H., Knittelfelder, O.L., Pieber, B., Rechberger,
25 G.N. *et al.* (2014) Regulation of gene expression through a transcriptional repressor
26 that senses acyl-chain length in membrane phospholipids. *Dev Cell* **29**: 729-739.
- 27 Hua, Z., Fatheddin, P., Graham, T.R. (2002) An essential subfamily of Drs2p-related P-
28 type ATPases is required for protein trafficking between Golgi complex and
29 endosomal/vacuolar system. *Mol Biol Cell* **13**: 3162-3177.
- 30
31 Huang, X., Withers, B.R., Dickson, R.C. (2014) Sphingolipids and lifespan regulation.
32 *Biochim Biophys Acta* **1841**: 657-664.
- 33 Hwang, S., Gustafsson, H.T., O'Sullivan, C., Bisceglia, G., Huang, X., Klose, C. *et al.*
34 (2017) Serine-dependent sphingolipid synthesis is a metabolic liability of aneuploid
35 cells. *Cell Rep* **21**: 3807-3818.
- 36
37 Jenkins, G.M., Richards, A., Wahl, T., Mao, C., Obeid, L., Hannun, Y. (1997)
38 Involvement of yeast sphingolipids in the heat stress response of *Saccharomyces*
39 *cerevisiae*. *J Biol Chem* **272**: 32566-32572.
- 40 Joutsen, J., Da Silva, A.J., Luoto, J.C., Budzynski, M.A., Nylund, A.S., de Thonel, A. *et*
41 *al.* (2020) Heat shock factor 2 protects against proteotoxicity by maintaining cell-cell
42 adhesion. *Cell Rep* **30**: 583-597.e6.
- 43
44 Jump, D.B., Torres-Gonzalez, M., Olson, L.K. (2011) Soraphen A, an inhibitor of acetyl
45 CoA carboxylase activity, interferes with fatty acid elongation. *Biochem Pharmacol*
46 **81**: 649-660.
- 47
48 Khakhina, S., Johnson, S.S., Manoharlal, R., Russo, S.B., Blugeon, C., Lemoine, S. *et*
49 *al.* (2015) Control of Plasma Membrane Permeability by ABC Transporters.
50 *Eukaryot Cell* **14**: 442-453.
- 51 Klose, C., Surma, M.A., Gerl, M.J., Meyenhofer, F., Shevchenko, A., Simons, K.
52 (2012) Flexibility of a eukaryotic lipidome--insights from yeast lipidomics. *PLoS*
53 *One* **7**: e35063.
- 54 Klug, L., Daum, G. (2014) Yeast lipid metabolism at a glance. *FEMS Yeast Res* **14**:
55 369-388.
- 56
57 Langmead, B., Salzberg, S.L. (2012) Fast gapped-read alignment with Bowtie 2. *Nat*
58 *Methods* **9**: 357-359.
- 59
60

- 1
2
3 Le Guédard, M., Bessoule, J.J., Boyer, V., Ayciriex, S., Velours, G., Kulik, W. (2009)
4 *PSII* is responsible for the stearic acid enrichment that is characteristic of
5 phosphatidylinositol in yeast. *FEBS J* **276**: 6412–6424.
- 6 Legras, J.L., Merdinoglu, D., Cornuet, J.M., Karst, F. (2007) Bread, beer and wine:
7 *Saccharomyces cerevisiae* diversity reflects human history. *Mol Ecol* **16**: 2091-2102.
- 8
9 | Legras, J.L., Galeote, V., Bigey, F., Camarasa, C., Marsit, S., Nidelet, T. *et al.* (2018)
10 Adaptation of *S. cerevisiae* to Fermented Food Environments Reveals Remarkable
11 Genome Plasticity and the Footprints of Domestication. *Mol Biol Evol* **35**: 1712-
12 1727.
- 13 Lester, R.L., Withers, B.R., Schultz, M.A., Dickson, R.C. (2013) Iron, glucose and
14 intrinsic factors alter sphingolipid composition as yeast cells enter stationary phase.
15 *Biochim Biophys Acta* **1831**: 726-736.
- 16
17 Li, H., Handsaker, B., Wysoker, A., Fennell, T., Ruan, J., Homer, N. *et al.* (2009) 1000
18 Genome Project Data Processing Subgroup. The Sequence alignment/map (SAM)
19 format and SAMtools. *Bioinformatics* **25**: 2078-2079.
- 20
21 Liu, G., Chen, Y., Færgeman, N.J., Nielsen, J. (2017) Elimination of the last reactions
22 in ergosterol biosynthesis alters the resistance of *Saccharomyces cerevisiae* to
23 multiple stresses. *FEMS Yeast Res* **17**(6), doi: 10.1093/femsyr/fox063.
- 24 López-Marqués, R.L., Holthuis, J.C., Pomorski, T.G. (2011) Pumping lipids with P4-
25 ATPases. *Biol Chem* **392**: 67-76.
- 26 Megyeri, M., Riezman, H., Schuldiner, M., Futerman, A.H. (2016) Making Sense of the
27 Yeast Sphingolipid Pathway. *J Mol Biol* **428**: 4765-4775.
- 28 Muthusamy, B.P., Natarajan, P., Zhou, X., Graham, T.R. (2009) Linking phospholipid
29 flippases to vesicle-mediated protein transport. *Biochim Biophys Acta* **1791**: 612-
30 619.
- 31
32 Oh, C.S., Toke, D.A., Mandala, S., Martin, C.E. (1997) *ELO2* and *ELO3*, homologues
33 of the *Saccharomyces cerevisiae* *ELO1* gene, function in fatty acid elongation and
34 are required for sphingolipid formation. *J Biol Chem* **272**: 17376-17384.
- 35 Okonechnikov, K., Conesa, A., García-Alcalde, F. (2016) Qualimap 2: advanced multi-
36 sample quality control for high-throughput sequencing data. *Bioinformatics* **32**: 292-
37 294.
- 38
39 Olson, D.K., Fröhlich, F., Christiano, R., Hannibal-Bach, H.K., Ejsing, C.S., Walther,
40 T.C. (2015) Rom2-dependent phosphorylation of Elo2 controls the abundance of
41 very long-chain fatty acids. *J Biol Chem* **290**: 4238–4247.
- 42 Oromendia, A.B., Dodgson, S.E., Amon, A. (2012) Aneuploidy causes proteotoxic
43 stress in yeast. *Genes Dev* **26**: 2696–2708.
- 44 Ouspenski, I.I., Elledge, S.J., Brinkley, B.R. (1999) New yeast genes important for
45 chromosome integrity and segregation identified by dosage effects on genome
46 stability. *Nucleic Acids Res* **27**: 3001–3008.
- 47
48 Pavelka, N., Rancati, G., Zhu, J., Bradford, W.D., Saraf, A., Florens, L. *et al.* (2010)
49 Aneuploidy confers quantitative proteome changes and phenotypic variation in
50 budding yeast. *Nature* **468**: 321-325.
- 51 Pérez-Torrado, R., Barrio, E., Querol, A. (2018) Alternative yeasts for winemaking:
52 *Saccharomyces non-cerevisiae* and its hybrids. *Crit Rev Food Sci Nutr* **58**: 1780-
53 1790.
- 54
55 Randez-Gil, F., Córcoles-Sáez, I., Prieto, J.A. (2013) Genetic and phenotypic
56 characteristics of baker's yeast: relevance to baking. *Annu Rev Food Sci Technol* **4**:
57 191-214.
- 58 Rodríguez-Vargas, S., Sánchez-García, A., Martínez-Rivas, J.M., Prieto, J.A., Randez-
59 Gil, F. (2007) Fluidization of membrane lipids enhances the tolerance of
60

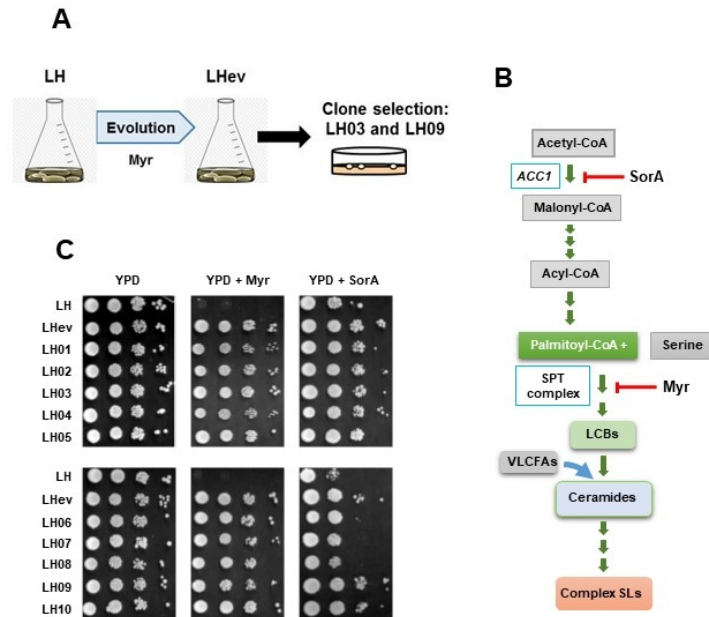
- 1
2
3 *Saccharomyces cerevisiae* to freezing and salt stress. *Appl Environ Microbiol* **73**:
4 110-116.
- 5 Rössler, H., Rieck, C., Delong, T., Hoja, U., Schweizer, E. (2003) Functional
6 differentiation and selective inactivation of multiple *Saccharomyces cerevisiae* genes
7 involved in very-long-chain fatty acid synthesis. *Mol Genet Genomics* **269**: 290-298.
- 8 Saito, K., Fujimura-Kamada, K., Furuta, N., Kato, U., Umeda, M., Tanaka, K. (2004)
9 Cdc50p, a protein required for polarized growth, associates with the Drs2p P-type
10 ATPase implicated in phospholipid translocation in *Saccharomyces cerevisiae*. *Mol*
11 *Biol Cell* **15**: 3418-3432.
- 12 Scott, A.L., Richmond, P.A., Dowell, R.D., Selmecki, A. (2017) The influence of
13 polyploidy on the evolution of yeast grown in a sub-optimal carbon source. *Mol Biol*
14 *Evol* **34**: 2690-2703.
- 15 Selmecki, A.M., Maruvka, Y.E., Richmond, P.A., Guillet, M., Shores, N., Sorenson,
16 A. *et al.* (2015) Polyploidy can drive rapid adaptation in yeast. *Nature* **519**: 349-352.
- 17 Sheltzer, J.M., Blank, H.M., Pfau, S.J., Tange, Y., George, B.M., Humpton, T.J. *et al.*
18 (2011) Aneuploidy drives genomic instability in yeast. *Science* **333**: 1026-1030.
- 19 Sicard, D., Legras, J.L. (2011) Bread, beer and wine: yeast domestication in the
20 *Saccharomyces sensu stricto* complex. *C R Biol* **334**: 229-236.
- 21 Storchová, Z., Breneman, A., Cande, J., Dunn, J., Burbank, K., O'Toole, E. *et al.* (2006)
22 Genome-wide genetic analysis of polyploidy in yeast. *Nature* **443**: 541-547.
- 23 Strucko, T., Zirngibl, K., Pereira, F., Kafkia, E., Mohamed, E.T., Rettel, M. *et al.* (2018)
24 Laboratory evolution reveals regulatory and metabolic trade-offs of glycerol
25 utilization in *Saccharomyces cerevisiae*. *Metab Eng* **47**: 73-82.
- 26 Sun, Y., Miao, Y., Yamane, Y., Zhang, C., Shokat, K.M., Takematsu, H. *et al.* (2012)
27 Orm protein phosphoregulation mediates transient sphingolipid biosynthesis
28 response to heat stress via the Pkh-Ypk and Cdc55-PP2A pathways. *Mol Biol Cell*
29 **23**: 2388-2398.
- 30 Tani, M., Kuge, O. (2012) Hydroxylation state of fatty acid and long-chain base
31 moieties of sphingolipid determine the sensitivity to growth inhibition due to *AURI*
32 repression in *Saccharomyces cerevisiae*. *Biochem Biophys Res Commun* **417**: 673-
33 678.
- 34 Tehlivets, O., Scheuringer, K., Kohlwein, S.D. (2007) Fatty acid synthesis and
35 elongation in yeast. *Biochim Biophys Acta* **1771**: 255-270.
- 36 Tenaillon, O., Barrick, J.E., Ribeck, N., Deatherage, D.E., Blanchard, J.L., Dasgupta, A.
37 *et al.* (2016) Tempo and mode of genome evolution in a 50,000-generation
38 experiment. *Nature* **536**: 165-170.
- 39 Toke, D.A., Martin, C.E. (1996) Isolation and characterization of a gene affecting fatty
40 acid elongation in *Saccharomyces cerevisiae*. *J Biol Chem* **271**: 18413-18422.
- 41 Torres, E. (2015) Yeast as Models of Mitotic Fidelity. *Recent Results Cancer Res* **200**:
42 143-164.
- 43 Torres, E.M., Sokolsky, T., Tucker, C.M., Chan, L.Y., Boselli, M., Dunham, M.J. *et al.*
44 (2007) Effects of aneuploidy on cellular physiology and cell division in haploid
45 yeast. *Science* **317**: 916-924.
- 46 Vahlensieck, H.F., Pridzun, L., Reichenbach, H., Hinnen, A. (1994) Identification of the
47 yeast *ACC1* gene product (acetyl-CoA carboxylase) as the target of the polyketide
48 fungicide soraphen A. *Curr Genet* **25**: 95-100.
- 49 Van den Bergh, B., Swings, T., Fauvart, M., Michiels, J. (2018) Experimental design,
50 population dynamics, and diversity in microbial experimental evolution. *Microbiol*
51 *Mol Biol Rev* **282**: e00008-18.
- 52
53
54
55
56
57
58
59
60

- 1
2
3
4
5
6
7
8
9
10
11
12
13
14
15
16
17
18
19
20
21
22
23
24
25
26
27
28
29
30
31
32
33
34
35
36
37
38
39
40
41
42
43
44
45
46
47
48
49
50
51
52
53
54
55
56
57
58
59
60
- Voordeckers, K., Kominek, J., Das, A., Espinosa-Cantú, A., De Maeyer, D., Arslan, A. *et al.* (2015) Adaptation to high ethanol reveals complex evolutionary pathways. *PLOS Genet* **11**: e1005635.
- Wadsworth, J.M., Clarke, D.J., McMahon, S.A., Lowther, J.P., Beattie, A.E., Langridge-Smith, P.R. *et al.* (2013) The chemical basis of serine palmitoyltransferase inhibition by myriocin. *J Am Chem Soc* **135**: 14276-14285.
- Weiß, C.L., Pais, M., Cano, L.M., Kamoun, S., Burbano, H. (2018) nQuire: a statistical framework for ploidy estimation using next generation sequencing. *BMC Bioinformatics* **19**: 122.
- Wenger, J.W., Piotrowski, J., Nagarajan, S., Chiotti, K., Sherlock, G., Rosenzweig, F. (2011) Hunger artists: yeast adapted to carbon limitation show trade-offs under carbon sufficiency. *PLoS Genet* **7**: e1002202.
- Yilancioglu, K., Weinstein, Z.B., Meydan, C., Akhmetov, A., Toprak, I., Durmaz, A. *et al.* (2014) Target-independent prediction of drug synergies using only drug lipophilicity. *J Chem Inf Model* **54**: 2286-2293.
- Zhu, J., Pavelka, N., Bradford, W.D., Rancati, G., Li, R. (2012) Karyotypic determinants of chromosome instability in aneuploid budding yeast. *PLoS Genet* **8**: e1002719.

Table 1. Likelihood ploidy by chromosome in the parental and evolved strains.

Chr.	Gene(*)	Likelihood ploidy		
		LH	LH03	LH09
I		tetra	di	tri
II		tetra	tetra	tetra
III	<i>ELO2</i>	tetra	tri	tetra
IV		tetra	tri	tri
V	<i>FAA2</i>	tetra	tri	tri
VI		tetra	tetra	tetra
VII	<i>ACB1</i>	tetra	tetra	tetra
VIII		tetra	tetra	tetra
IX	<i>FAA3</i>	tetra	tetra	tetra
X	<i>ELO1</i>	tetra	tri	tetra
XI	<i>FAS1</i>	tetra	tetra	tetra
XII	<i>ELO3</i>	tetra	tri	tetra
XIII	<i>SCS7, FAA4</i>	tetra	tri	tetra
XIV		tetra	tri	tetra
XV	<i>FAA1</i>	tetra	tetra	tetra
XVI	<i>FAS2</i>	tetra	tri	tetra

(*) Relevant lipid metabolism gene included in this chromosome



45 **Fig. 1.** The adaptive evolution experiment, its metabolic context, and initial characterization of the evolved
 46 population. (A) Schematic representation of the myriocin-driven evolution approach. (B) Main metabolic
 47 steps involved in the synthesis of complex SLs from acetyl-CoA. The red arrows indicate the enzymes
 48 inhibited by myriocin (SPT) and soraphen A (Acc1). For more details see text and important reviews (Henry
 49 *et al.*, 2012; Klug and Daum, 2014; Huang *et al.*, 2014; Megyeri *et al.*, 2016). (C) Growth of the parental
 50 strain LH, 50-generation evolved population LHev and isolated clones LH03 and LH09, was assayed at 30°C
 51 in the absence (YPD) or presence of 1.2 μM myriocin (YPD + Myr) or 0.25 μg/ml soraphen A (YPD + SorA).
 In all cases, cells were pre-grown and treated as described in the Material and methods section.

52 190x275mm (96 x 96 DPI)

53
54
55
56
57
58
59
60

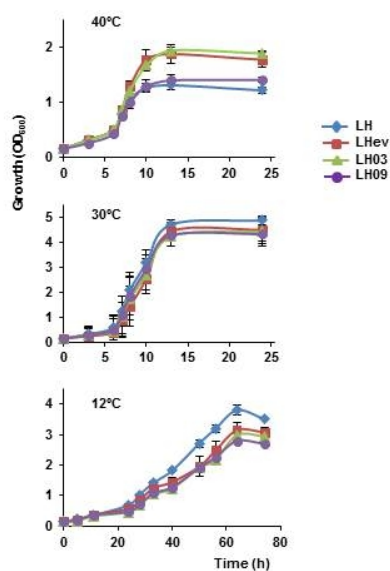


Fig. 2. Growth at different temperatures of the evolved populations. Cells of the parental LH strain, evolved population LHev and isolated clones LH00-LH10 were pre-grown in liquid SCD medium, refreshed in the same medium (initial OD₆₀₀ ~ 0.5) and their growth at 12, 30 or 40°C was followed for the indicated time. Data represent the mean value (\pm SD) of three biological replicates.

190x254mm (96 x 96 DPI)

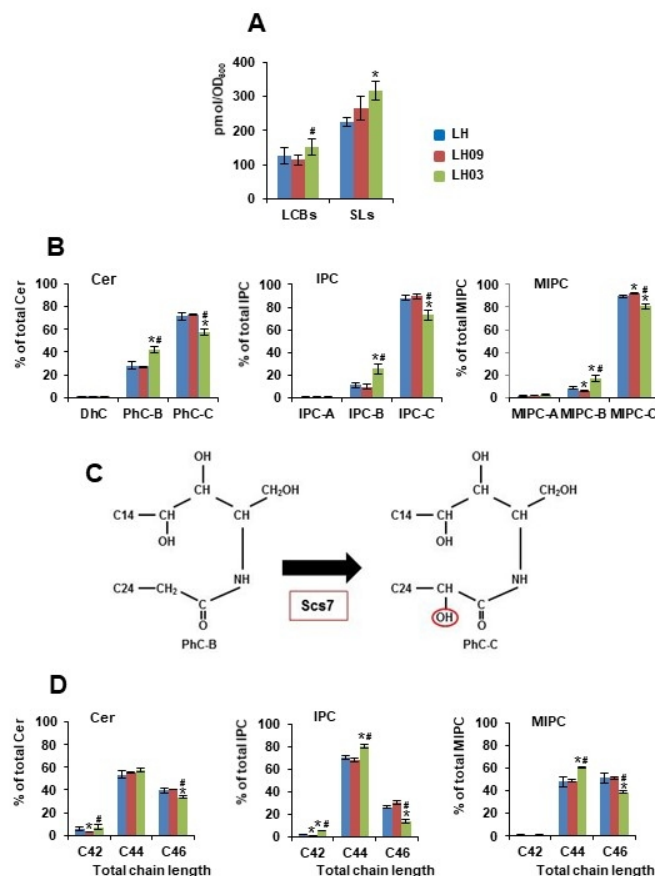


Fig. 3. Myriocin-driven adaptive evolution alters SLs composition. (A) The relative content of LCBs and SLs in YPD-grown cells ($OD_{600} \sim 1.0$) of the LH, LH03 and LH09 strains was analysed by UPLC. Sphinganine (d17:0) and C12 Ceramide (d18:1/12:0), were used as internal standards of LCBs and SLs, respectively. The levels of the different lipid species in each sample were normalized to the corresponding internal standard (pmol eq) and units of processed cells (OD_{600}). Phosphorylated LCBs were below the detection limit. The quantity of SLs represents the sum of Cer, IPC and MIPC. (B) The amount of Cer, IPC and MIPC sub-classes were normalized (%) to the total content of each class. (C) Hydroxylation of phytoceramide (PhC-B) by Scs7 generates α -OH-phytoceramide (PhC-C). These Cer sub-classes are then converted to the corresponding IPC-B and IPC-C, and subsequently to MIPC-B and MIPC-C, respectively. For more details see important reviews (Huang *et al.*, 2014; Megyeri *et al.*, 2016). (D) The quantities of Cer, IPC and MIPC species containing the same number of carbon atoms are summed and these values were normalized (%) to the total amount of the corresponding SLs class. In all cases, the data were calculated from at least three biological replicates (\pm SD). Statistically significant differences ($p < 0.05$) between LH and LH03 or LH09

1
2
3 samples (*), and between the evolved clones LH03 and LH09 (#) are indicated.
4

5 190x254mm (96 x 96 DPI)
6
7
8
9
10
11
12
13
14
15
16
17
18
19
20
21
22
23
24
25
26
27
28
29
30
31
32
33
34
35
36
37
38
39
40
41
42
43
44
45
46
47
48
49
50
51
52
53
54
55
56
57
58
59
60

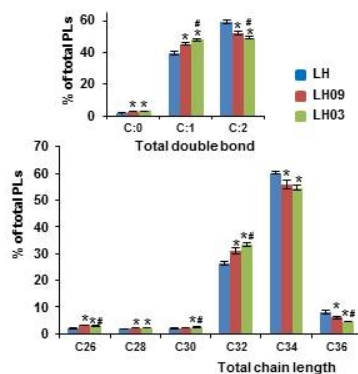


Fig. 4. The total acyl chain length and the unsaturation degree of PLs are affected in response to chronic myriocin exposure. The quantities of the PLs species containing the same number of double bonds or the same number of carbon atoms in the hydrocarbon moiety are summed and these values were normalized to the total amount of PLs (%). Statistically significant differences ($p < 0.05$) between LH and LH03 or LH09 samples (*), and between the evolved clones LH03 and LH09 (#) are indicated. Data represent the mean value (\pm SD) of three independent biological replicates.

190x254mm (96 x 96 DPI)

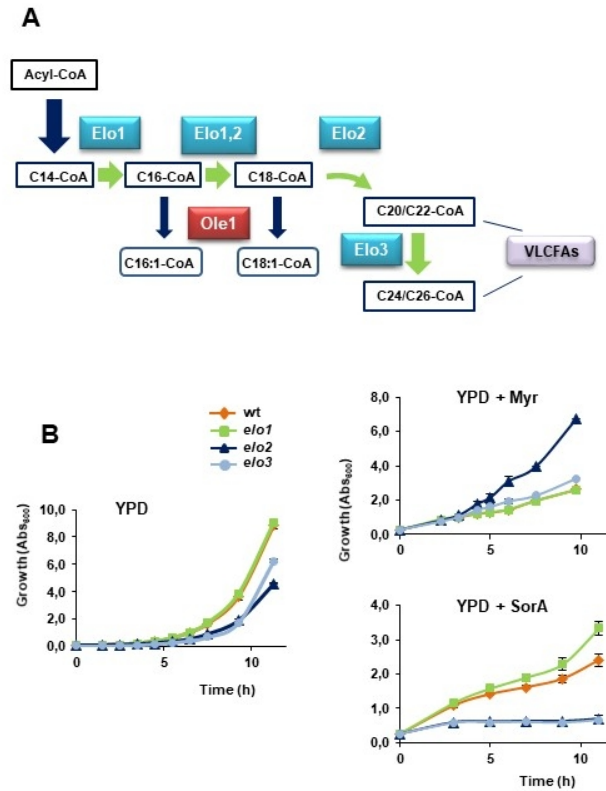


Fig. 5. Impaired fatty acid elongation affects growth of yeast cells on myriocin and soraphen A. (A) Schematic representation of fatty acids elongation and desaturation in the yeast endoplasmic reticulum (ER). The reactions scheme up to C26 and the elongases involved, Elo1, Elo2 and Elo3 are shown. Fatty acids are monounsaturated via a reaction catalysed by the ER-resident and essential $\Delta 9$ desaturase, Ole1. For more details see representative reviews (Tehlivets *et al.*, 2007; Henry *et al.*, 2012; Klug and Daum, 2014; Huang *et al.*, 2014; Megyeri *et al.*, 2016). (B) Cells of the laboratory wild-type BY4741 strain (wt) and its corresponding elongase mutants, *elo1*, *elo2* and *elo3*, were pre-grown in liquid YPD medium, refreshed in the same medium (initial OD₆₀₀ ~ 0.05) lacking (YPD) or containing 2.0 μ M myriocin (YPD + Myr) or 0.25 μ g/ml soraphen A (YPD + SorA), and their growth was followed for the indicated time. Data represent the mean value (\pm SD) of three biological replicates.

190x254mm (96 x 96 DPI)

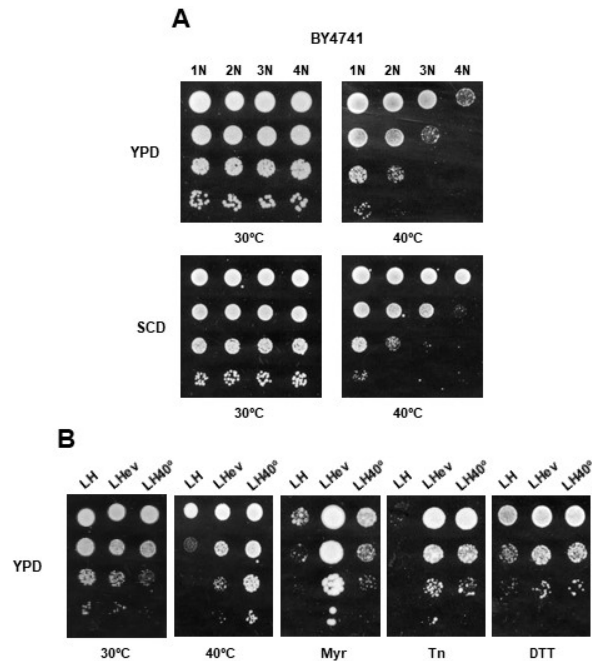


Fig. 6. Ploidy effects and phenotypic variation of myriocin- and heat-evolved terminal populations. (A) A series of isogenic BY4741-derivative strains differing in ploidy level (1N, 2N, 3N and 4N; Storchová *et al.*, 2006) were analysed for growth. Ten-fold serial dilutions of saturated cultures grown in minimal SCD or rich YPD medium were prepared and 3 μ l aliquots of three dilutions (10^{-1} – 10^{-3}) were applied over SCD- or YPD-agar-gelled plates. Colony growth was inspected after 2 days of incubation at 30°C or 40°C. (B) Growth of the myriocin-(LH^{ev}) and heat-evolved (LH40⁰) terminal populations of the industrial parental strain L'Hirondelle (LH), was assayed at 40°C or at 30°C in the absence (YPD) or presence of 0.75 μ M myriocin (Myr), 0.4 mM tunicamycin (Tn) or 5 μ M DTT (DTT). In all cases, cells were pre-grown at 30°C or 40°C and treated as described above. In all cases, a representative experiment is shown.

190x254mm (96 x 96 DPI)

Supplementary information

Myriocin-induced adaptive laboratory evolution of an industrial strain of *Saccharomyces cerevisiae* reveals its potential to remodel lipid composition and heat tolerance

Francisca Randez-Gil, Jose A. Prieto, Alejandro Rodríguez-Puchades, Josefina Casas, Vicente Sentandreu and Francisco Estruch

Contents:

Fig. S1-S4

Tables S1-S15

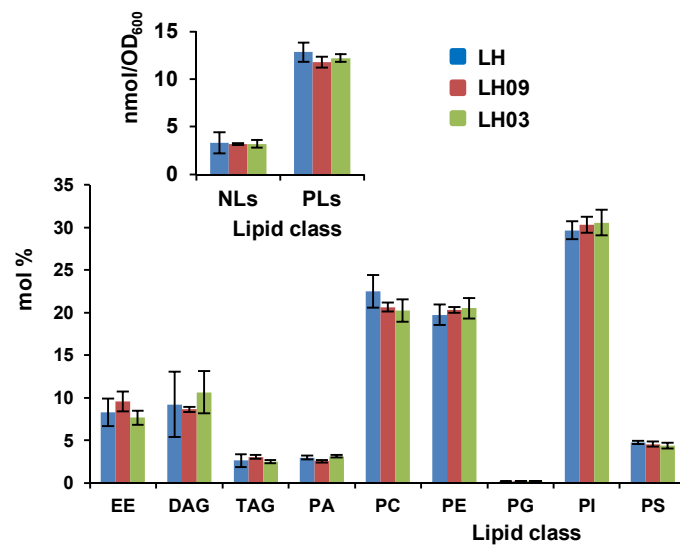


Fig. S1. NLs and PLs abundance. Lipid profiles of the parental LH and the evolved clones LH03 and LH09 in YPD were analysed for neutral lipids (NLs) and phospholipids (PLs) classes. 30°C-grown ($OD_{600} \sim 1.0$) cells were analysed by mass-spectrometry-based shotgun lipidomics. The amount of NLs, PLs, and their corresponding classes were normalized to the total lipid content and expressed as the mol%. Data represent the mean value (\pm SD) of three independent biological replicates. More details are given in the Experimental procedures section.

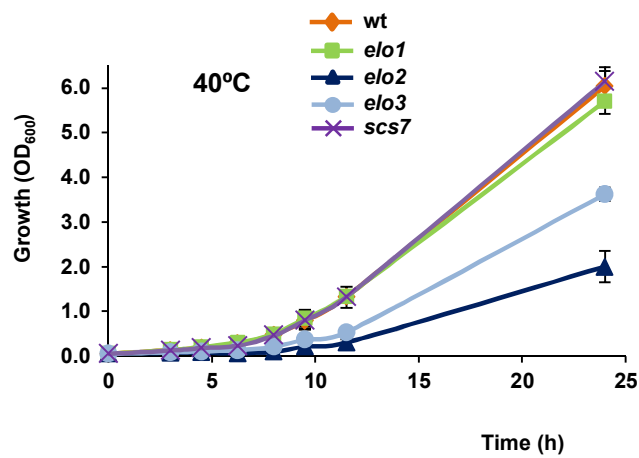


Fig. S2. Knock-out of some elongase genes depresses growth of yeast cells at high temperature. Cells of the laboratory wild-type BY4741 strain (wt) and its corresponding elongase mutants, *elo1*, *elo2* and *elo3*, were pre-grown in liquid YPD medium, refreshed in the same medium (initial OD₆₀₀ ~ 0.05) and their growth was followed at 40°C for the indicated time. Growth of the hydroxylase mutant *scs7* is also shown. Data represent the mean value (\pm SD) of three biological replicates.

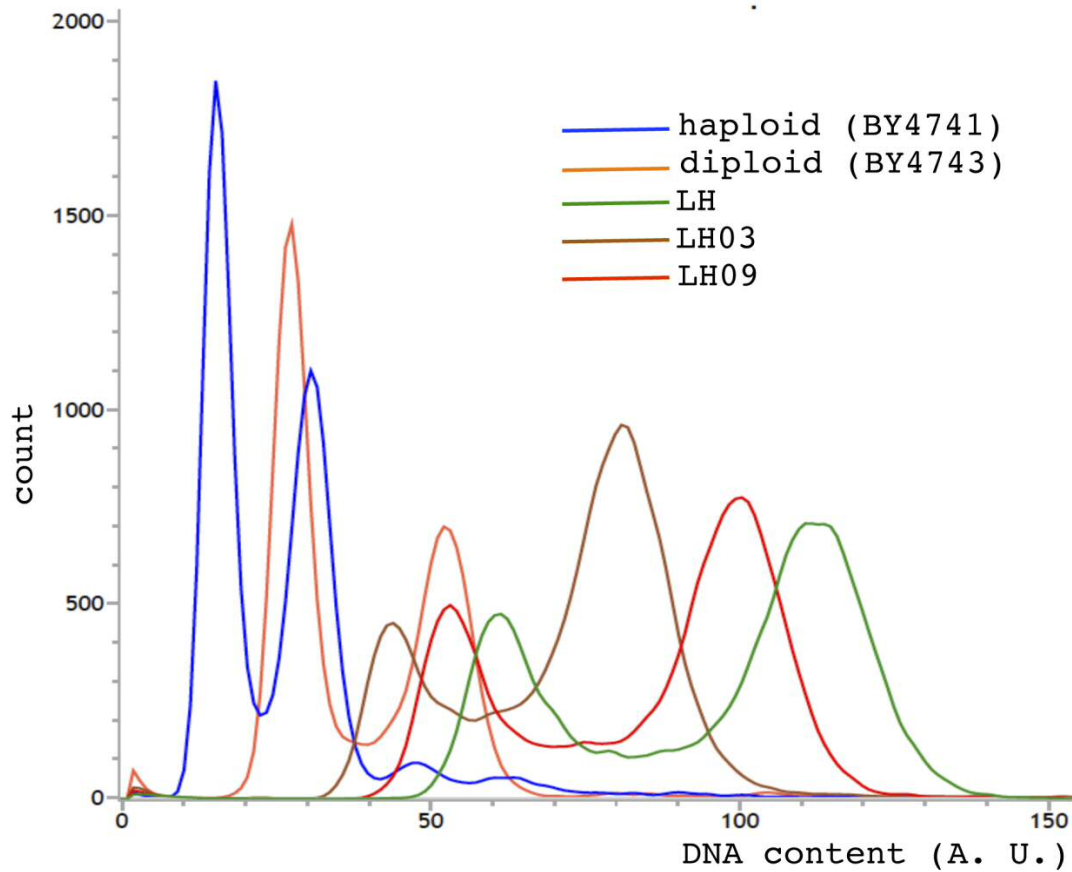


Fig. S3. Histogram of cell count by DNA content of experimental populations. The industrial LH strain and the evolved clones LH03 and LH09 were analysed for ploidy level by flow cytometry. Strains of known ploidy size, BY4741 (1N) and BY4743 (2N) were used as a genome size control. More details are given in the Experimental procedures section. A representative experiment is shown.

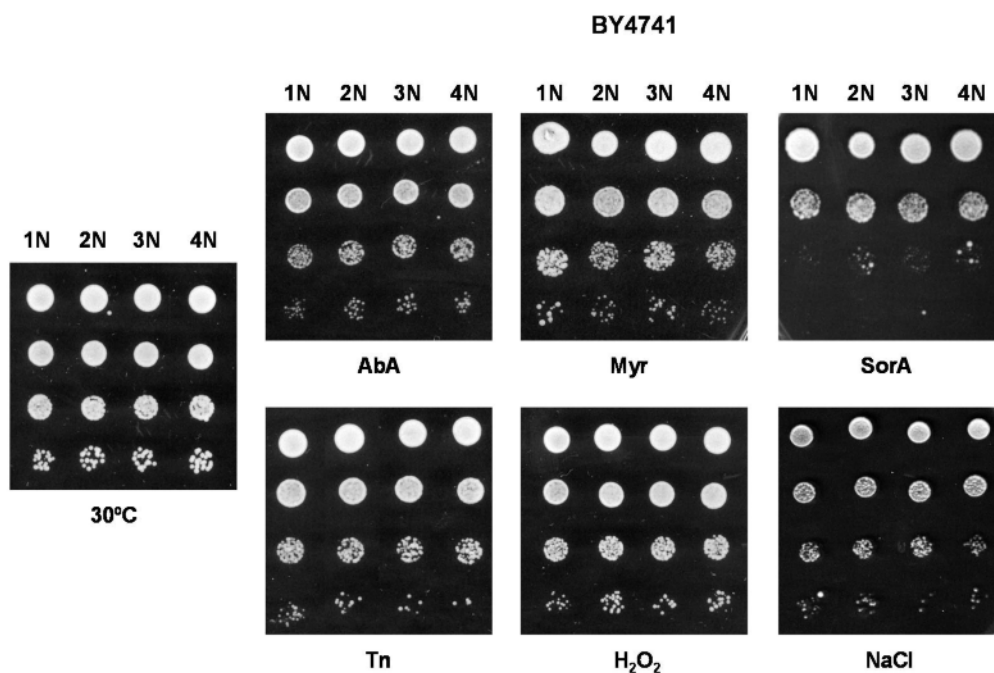


Fig. S4. Ploidy-specific growth effects under different stressful conditions. A series of isogenic BY4741-derivative strains differing in ploidy level (1N, 2N, 3N and 4N; Storchová *et al.*, 2006) were analysed for growth. Cells were grown in minimal SCD medium to the mid-exponential phase at 30°C ($OD_{600} \sim 0.5$). Then, 10-fold serial dilutions were prepared and 3 μ l aliquots of three dilutions (10^{-1} – 10^{-3}) were applied over SCD agar-gelled plates containing 2 μ M aureobasidin A (AbA), 1.2 μ M myriocin (Myr), 0.25 μ g/ml soraphen A (SorA), 0.4 μ M tunicamycin (Tn), 2 μ M H₂O₂ (H₂O₂) or 1.0 M NaCl (NaCl). Colony growth was inspected after 2-4 days of incubation at 30°C. In all cases, a representative experiment is shown.

TABLE S1. Relative abundance of Cer molecular species found in the parental yeast strain LH and their corresponding myriocin-evolved clones LH09 and LH03.

Cer specie	% of total Cer class \pm SD ^a		
	LH	LH09	LH03
DhC			
DhC (d18:0/20:0)	0.03 \pm 0.00	0.02 \pm 0.00	0.04 \pm 0.01 ^{*#}
DhC (d18:0/22:0)	0.06 \pm 0.01	0.05 \pm 0.01	0.06 \pm 0.01
DhC (d18:0/24:0)	0.24 \pm 0.02	0.16 \pm 0.02 [*]	0.24 \pm 0.03 [#]
PhC-B			
PhC (t32:0)	0.01 \pm 0.00	nd	0.02 \pm 0.01 [*]
PhC (t34:0)	0.06 \pm 0.00	0.05 \pm 0.00 [*]	0.10 \pm 0.01 ^{*#}
PhC (t36:0)	0.10 \pm 0.02	0.07 \pm 0.01 [*]	0.17 \pm 0.01 ^{*#}
PhC (t38:0)	0.11 \pm 0.01	0.07 \pm 0.00 [*]	0.16 \pm 0.02 ^{*#}
PhC (t40:0)	0.12 \pm 0.01	0.07 \pm 0.01 [*]	0.19 \pm 0.06 [#]
PhC (t42:0)	1.33 \pm 0.14	0.73 \pm 0.11 [*]	2.39 \pm 0.58 ^{*#}
PhC (t44:0)	14.34 \pm 1.65	14.62 \pm 0.22	23.53 \pm 0.99 ^{*#}
PhC (t46:0)	12.05 \pm 1.56	11.14 \pm 0.67	15.65 \pm 1.65 ^{*#}
PhC-C			
PhC (t34:0(2OH))	0.04 \pm 0.01	0.04 \pm 0.00	0.03 \pm 0.00 ^{*#}
PhC (t36:0(2OH))	0.07 \pm 0.01	0.05 \pm 0.01	0.04 \pm 0.00 ^{*#}
PhC (t38:0(2OH))	0.05 \pm 0.02	0.05 \pm 0.01	0.05 \pm 0.02
PhC (t40:0(2OH))	0.11 \pm 0.03	0.07 \pm 0.00 [*]	0.09 \pm 0.02
PhC (t42:0(2OH))	4.40 \pm 1.40	2.52 \pm 0.35 [*]	4.88 \pm 1.53 [#]
PhC (t44:0(2OH))	39.36 \pm 3.30	40.70 \pm 0.93	34.16 \pm 2.33 ^{*#}
PhC (t46:0(2OH))	27.53 \pm 2.06	29.57 \pm 0.39	18.21 \pm 1.43 ^{*#}

^a Values are mean \pm SD of three independent replicates. Significance level: ^{*,#} $p < 0.05$. ^{*} Significant difference of LH03 or LH09 compared with LH. [#] Significant difference of LH03 compared with LH09. nd, non detected.

TABLE S2. Relative abundance of IPC molecular species found in the parental yeast strain LH and their corresponding myriocin-evolved clones LH09 and LH03.

IPC specie	% of total IPC class \pm SD ^a		
	LH	LH09	LH03
IPC-A			
IPC (d38:0)	nd	nd	nd
IPC (d40:0)	nd	nd	nd
IPC (d42:0)	nd	nd	nd
IPC (d44:0)	0.62 \pm 0.06	0.60 \pm 0.05	0.88 \pm 0.18 ^{*#}
IPC (d46:0)	nd	nd	nd
IPC-B			
IPC (t38:0)/IPC (d38:0(2OH))	nd	nd	nd
IPC (t40:0)/IPC (d40:0(2OH))	nd	nd	nd
IPC (t42:0)/IPC (d42:0(2OH))	0.41 \pm 0.07	0.19 \pm 0.03 [*]	1.46 \pm 0.55 ^{*#}
IPC (t44:0)/IPC (d44:0(2OH))	10.73 \pm 2.15	9.67 \pm 1.85	24.32 \pm 4.10 ^{*#}
IPC (t46:0)/IPC (d46:0(2OH))	nd	nd	nd
IPC-C			
IPC (t38:0(2OH))	0.11 \pm 0.04	0.06 \pm 0.02	0.08 \pm 0.04
IPC (t40:0(2OH))	nd	nd	nd
IPC (t42:0(2OH))	2.50 \pm 0.08	1.29 \pm 0.10 [*]	3.52 \pm 0.89 [*]
IPC (t44:0(2OH))	58.56 \pm 2.79	58.33 \pm 0.39	53.90 \pm 2.14 ^{*#}
IPC (t46:0(2OH))	27.08 \pm 1.27	29.86 \pm 1.41	15.84 \pm 3.76 ^{*#}

^a Values are mean \pm SD of three independent replicates. Significance level: ^{*,#} $p < 0.05$. ^{*} Significant difference of LH03 or LH09 compared with LH. [#] Significant difference of LH03 compared with LH09. nd, non detected.

TABLE S3. Relative abundance of MIPC molecular species found in the parental yeast strain LH and their corresponding myriocin-evolved clones LH03 and LH09.

MIPC specie	% of total MIPC class \pm SD ^a		
	LH	LH09	LH03
MIPC-A			
MIPC (d38:0)	nd	nd	nd
MIPC (d40:0)	nd	nd	nd
MIPC (d42:0)	0.22 \pm 0.05	nd	0.41 \pm 0.11*
MIPC (d44:0)	2.82 \pm 0.53	2.61 \pm 0.18	4.45 \pm 0.63* [#]
MIPC (d46:0)	1.36 \pm 0.32	1.24 \pm 0.35	1.62 \pm 0.79
MIPC-B			
MIPC (t38:0)/MIPC (d38:0(2OH))	nd	nd	nd
MIPC (t40:0)/MIPC (d40:0(2OH))	nd	nd	nd
MIPC (t42:0)/MIPC (d42:0(2OH))	0.55 \pm 0.18	0.40 \pm 0.05	0.36 \pm 0.12
MIPC (t44:0)/MIPC (d44:0(2OH))	8.11 \pm 1.26	5.83 \pm 0.58*	16.84 \pm 2.47* [#]
MIPC (t46:0)/MIPC (d46:0(2OH))	19.76 \pm 5.01	14.51 \pm 1.85	27.44 \pm 4.78 [#]
MIPC-C			
MIPC (t38:0(2OH))	nd	nd	nd
MIPC (t40:0(2OH))	nd	nd	nd
MIPC (t42:0(2OH))	0.31 \pm 0.02	nd	0.32 \pm 0.07
MIPC (t44:0(2OH))	48.53 \pm 3.35	49.54 \pm 2.92	53.02 \pm 4.38
MIPC (t46:0(2OH))	40.87 \pm 3.33	42.37 \pm 3.17	27.24 \pm 5.58* [#]

^a Values are mean \pm SD of three independent replicates. Significance level: *[#] $p < 0.05$. * Significant difference of LH03 or LH09 compared with LH. [#] Significant difference of LH03 compared with LH09. nd, non detected.

TABLE S4. Composition, chain length and degree of unsaturation of TAG molecular species found in the parental yeast strain LH and their corresponding myriocin-evolved clones LH03 and LH09.

TAG specie	mol % of total TAG \pm SD ^a		
	LH	LH09	LH03
C42:1	2.25 \pm 1.59	4.19 \pm 0.38	4.85 \pm 0.19 [#]
C42:2	3.14 \pm 0.46	3.87 \pm 0.13 [*]	4.12 \pm 2.38
C44:2	4.07 \pm 0.49	4.45 \pm 0.22	4.84 \pm 0.23 [*]
C48:3	13.23 \pm 0.83	16.00 \pm 0.71 [*]	17.92 \pm 1.01 ^{**}
C50:3	42.89 \pm 1.64	41.63 \pm 1.22	41.42 \pm 0.48
C52:3	32.06 \pm 2.83	24.31 \pm 1.11 [*]	22.37 \pm 1.51 [*]
C56:1	nd	2.56 \pm 1.57	1.37 \pm 0.79
C56:2	2.39 \pm 1.69	2.48 \pm 1.44	2.12 \pm 1.23
C56:3	1.70 \pm 0.16	1.58 \pm 0.93	1.53 \pm 0.88
C58:1	nd	1.49 \pm 0.86	1.17 \pm 0.68
C58:2	1.18 \pm 0.84	1.92 \pm 1.11	2.28 \pm 1.34
C60:2	nd	nd	3.41 \pm 1.97
Total chain length			
C42	4.27 \pm 1.13	8.06 \pm 0.45 [*]	8.86 \pm 0.20 [*]
C44	4.07 \pm 0.49	4.45 \pm 0.22	4.84 \pm 0.23 [*]
C48	13.23 \pm 0.83	16.00 \pm 0.71 [*]	17.92 \pm 1.01 ^{**}
C50	42.89 \pm 1.64	41.63 \pm 1.22	41.42 \pm 0.48
C52	32.06 \pm 2.83	24.31 \pm 1.11 [*]	22.37 \pm 1.51 [*]
C56	2.89 \pm 1.85	6.63 \pm 0.42	2.51 \pm 1.62 [#]
C58	1.18 \pm 0.68	3.41 \pm 1.97	2.87 \pm 1.19
C60	nd	nd	3.41 \pm 0.14
Degree of unsaturation			
C:1	3.17 \pm 2.05	6.39 \pm 1.04 [*]	5.70 \pm 0.56 [*]
C:2	9.33 \pm 1.40	10.62 \pm 0.38	12.08 \pm 0.62 ^{**}
C:3	88.55 \pm 2.31	82.99 \pm 1.38 [*]	82.22 \pm 0.63 [*]

^a Values are mean \pm SD of three independent replicates. Significance level: ^{*}[#] $p < 0.05$. ^{*} Significant difference of LH03 or LH09 compared with LH. [#] Significant difference of LH03 compared with LH09. nd, non detected.

TABLE S5. Composition, chain length and degree of unsaturation of SE molecular species found in the parental yeast strain LH and their corresponding myriocin-evolved clones LH03 and LH09.

SE specie	mol % of total SE \pm SD ^a		
	LH	LH09	LH03
C16:0	25.33 \pm 2.13	26.55 \pm 2.51	26.06 \pm 2.22
C16:1	40.44 \pm 3.03	41.26 \pm 1.47	46.09 \pm 2.18
C18:0	34.23 \pm 0.90	32.19 \pm 3.98	27.85 \pm 0.04 [*]
Total chain length			
C16	65.77 \pm 0.90	67.81 \pm 3.98	72.15 \pm 0.04
C18	34.23 \pm 0.90	32.19 \pm 3.98	27.85 \pm 0.04 [*]
Degree of unsaturation			
C:0	25.33 \pm 2.13	26.55 \pm 2.51	26.06 \pm 2.22
C:1	74.67 \pm 2.13	73.45 \pm 2.51	73.94 \pm 2.22

^a Values are mean \pm SD of three independent replicates. Significance level: ^{*},[#] $p < 0.05$. ^{*} Significant difference of LH03 or LH09 compared with LH. [#] Significant difference of LH03 compared with LH09.

TABLE S6. Composition, chain length and degree of unsaturation of DAG molecular species found in the parental yeast strain LH and their corresponding myriocin-evolved clones LH03 and LH09.

DAG specie	mol % of total DAG \pm SD ^a		
	LH	LH09	LH03
C30:2	0.72 \pm 0.30	0.43 \pm 0.06	0.51 \pm 0.08
C32:1	12.76 \pm 0.43	17.36 \pm 0.67 [*]	19.25 \pm 0.29 ^{*#}
C32:2	16.35 \pm 0.00	19.62 \pm 0.18 [*]	19.10 \pm 0.52 [*]
C34:1	31.71 \pm 1.82	32.52 \pm 0.57	33.41 \pm 0.42 [#]
C34:2	32.64 \pm 3.34	30.07 \pm 1.28	27.73 \pm 0.76 ^{*#}
C36:2	5.82 \pm 0.79	nd	
Total chain length			
C30	0.72 \pm 0.30	0.43 \pm 0.06	0.51 \pm 0.08
C32	29.11 \pm 0.42	36.98 \pm 0.78 [*]	38.35 \pm 0.80 [*]
C34	64.35 \pm 1.52	62.59 \pm 0.83	61.14 \pm 0.86 [*]
C36	5.82 \pm 0.79	nd	
Degree of unsaturation			
C:1	44.47 \pm 2.25	49.88 \pm 1.16 [*]	52.66 \pm 0.37 ^{*#}
C:2	55.53 \pm 2.25	50.12 \pm 1.16 [*]	47.34 \pm 0.37 ^{*#}

^a Values are mean \pm SD of three independent replicates. Significance level: ^{*,#} $p < 0.05$. ^{*} Significant difference of LH03 or LH09 compared with LH. [#] Significant difference of LH03 compared with LH09. nd, non detected.

TABLE S7. Composition, chain length and degree of unsaturation of PA molecular species found in the parental yeast strain LH and their corresponding myriocin-evolved clones LH03 and LH09.

PA specie	mol % of total PA \pm SD ^a		
	LH	LH09	LH03
C28:1	1.82 \pm 0.27	nd	1.85 \pm 0.21
C30:1	1.92 \pm 0.17	2.11 \pm 0.09	2.54 \pm 0.12 ^{*#}
C30:2	1.58 \pm 0.01	nd	1.15 \pm 0.07 [*]
C32:1	7.89 \pm 0.56	11.77 \pm 0.61 [*]	12.53 \pm 0.57 [*]
C32:2	27.49 \pm 1.07	27.10 \pm 0.50	27.52 \pm 1.30
C34:1	15.30 \pm 0.20	19.08 \pm 1.15 [*]	21.01 \pm 1.75 [*]
C34:2	41.67 \pm 0.89	37.47 \pm 1.65 [*]	32.32 \pm 0.26 ^{*#}
C36:2	3.47 \pm 0.29	2.46 \pm 0.55 [*]	1.47 \pm 0.04 ^{*#}
Total chain length			
C28	1.82 \pm 0.27	nd	1.85 \pm 0.21
C30	2.97 \pm 0.74	2.11 \pm 0.09	3.31 \pm 0.76
C32	35.37 \pm 1.43	38.88 \pm 1.01 [*]	40.05 \pm 1.20 [*]
C34	56.97 \pm 1.07	56.55 \pm 0.52	53.32 \pm 1.50 ^{*#}
C36	3.47 \pm 0.29	2.46 \pm 0.55 [*]	1.47 \pm 0.04 ^{*#}
Degree of unsaturation			
C:1	26.31 \pm 0.79	32.97 \pm 1.83 [*]	37.93 \pm 1.97 ^{*#}
C:2	73.69 \pm 0.79	67.03 \pm 1.83 [*]	62.07 \pm 1.97 ^{*#}

^a Values are mean \pm SD of three independent replicates. Significance level: ^{*,#} $p < 0.05$. ^{*} Significant difference of LH03 or LH09 compared with LH. [#] Significant difference of LH03 compared with LH09. nd, non detected.

TABLE S8. Composition, chain length and degree of unsaturation of PC molecular species found in the parental yeast strain LH and their corresponding myriocin-evolved clones LH03 and LH09.

PC specie	mol % of total PC \pm SD ^a		
	LH	LH09	LH03
C26:0	0.28 \pm 0.07	0.47 \pm 0.01 [*]	0.47 \pm 0.04 [*]
C26:1	2.79 \pm 1.61	3.81 \pm 2.20 [*]	3.34 \pm 0.06 ^{*#}
C26:2	0.09 \pm 0.01	0.09 \pm 0.00	0.06 \pm 0.00 ^{*#}
C28:0	0.09 \pm 0.06	0.21 \pm 0.00 [*]	0.24 \pm 0.02 ^{*#}
C28:1	2.48 \pm 0.08	2.90 \pm 0.07 [*]	2.98 \pm 0.10 [*]
C28:2	0.08 \pm 0.04	0.07 \pm 0.01	0.06 \pm 0.01 ^{*#}
C30:0	nd	0.05 \pm 0.01	0.08 \pm 0.01 [#]
C30:1	1.68 \pm 0.17	2.37 \pm 0.08 [*]	3.05 \pm 0.05 ^{*#}
C30:2	1.60 \pm 0.17	1.34 \pm 0.07 [*]	1.45 \pm 0.09
C32:1	2.73 \pm 0.56	5.49 \pm 0.29 [*]	6.20 \pm 0.43 ^{*#}
C32:2	36.98 \pm 1.45	38.59 \pm 0.45	43.03 \pm 0.59 ^{*#}
C34:1	1.18 \pm 0.21	2.30 \pm 0.09 [*]	2.55 \pm 0.20 [*]
C34:2	44.53 \pm 1.40	38.73 \pm 2.14 [*]	33.29 \pm 0.31 ^{*#}
C36:1	0.56 \pm 0.12	0.63 \pm 0.03	0.68 \pm 0.04
C36:2	5.77 \pm 0.40	4.12 \pm 0.54 [*]	2.47 \pm 0.05 ^{*#}
C38:2	0.15 \pm 0.01	0.09 \pm 0.01 [*]	0.05 \pm 0.00 ^{*#}
Total chain length			
C26	3.20 \pm 1.85	4.36 \pm 2.52 [*]	3.87 \pm 0.03 ^{*#}
C28	2.60 \pm 0.13	3.18 \pm 0.08 [*]	3.28 \pm 0.11 [*]
C30	3.28 \pm 0.09	3.76 \pm 0.08 [*]	4.58 \pm 0.12 ^{*#}
C32	39.71 \pm 1.16	44.09 \pm 0.72 [*]	49.23 \pm 0.32 ^{*#}
C34	45.71 \pm 1.19	41.03 \pm 2.13 [*]	35.84 \pm 0.24 ^{*#}
C36	6.33 \pm 0.43	4.75 \pm 0.57 [*]	3.14 \pm 0.04 ^{*#}
C38	0.16 \pm 0.02	0.26 \pm 0.02 [*]	0.33 \pm 0.02 ^{*#}
Degree of unsaturation			
C:0	0.34 \pm 0.12	0.73 \pm 0.01 [*]	0.79 \pm 0.05 [*]
C:1	10.49 \pm 2.61	16.24 \pm 2.34 [*]	18.80 \pm 0.70 [*]
C:2	89.17 \pm 2.73	83.03 \pm 2.33 [*]	80.41 \pm 0.75 [*]

^a Values are mean \pm SD of three independent replicates. Significance level: ^{*},[#] $p < 0.05$. ^{*} Significant difference of LH03 or LH09 compared with LH. [#] Significant difference of LH03 compared with LH09. nd, non detected.

TABLE S9. Composition, chain length and degree of unsaturation of PE molecular species found in the parental yeast strain LH and their corresponding myriocin-evolved clones LH03 and LH09.

PE specie	mol % of total PE \pm SD ^a		
	LH	LH09	LH03
C26:0	0.16 \pm 0.09	0.29 \pm 0.17	0.27 \pm 0.03
C26:1	0.18 \pm 0.10	0.27 \pm 0.15	0.19 \pm 0.03
C28:0	nd	0.16 \pm 0.09	0.16 \pm 0.09
C28:1	0.31 \pm 0.18	0.36 \pm 0.05	0.33 \pm 0.03
C30:1	0.67 \pm 0.09	0.79 \pm 0.01 [*]	0.91 \pm 0.08 ^{*#}
C32:1	6.91 \pm 0.37	9.61 \pm 0.58 [*]	11.73 \pm 0.08 ^{*#}
C32:2	11.24 \pm 0.38	14.12 \pm 0.66 [*]	14.49 \pm 0.16 [*]
C34:1	14.38 \pm 1.21	16.02 \pm 0.38 [*]	17.74 \pm 0.45 ^{*#}
C34:2	58.36 \pm 0.89	51.82 \pm 1.00 [*]	50.02 \pm 0.26 ^{*#}
C36:2	8.12 \pm 0.59	7.05 \pm 0.28 [*]	4.21 \pm 0.10 ^{*#}
Total chain length			
C26	0.17 \pm 0.10	0.55 \pm 0.32	0.46 \pm 0.02
C28	0.31 \pm 0.18	0.42 \pm 0.13	0.44 \pm 0.10
C30	0.67 \pm 0.09	0.79 \pm 0.01 [*]	0.91 \pm 0.08 ^{*#}
C32	18.15 \pm 0.24	23.73 \pm 1.22 [*]	26.22 \pm 0.18 ^{*#}
C34	72.74 \pm 0.49	67.83 \pm 1.24 [*]	67.77 \pm 0.21 [*]
C36	8.12 \pm 0.59	7.05 \pm 0.28 [*]	4.21 \pm 0.10 ^{*#}
Degree of unsaturation			
C:0	0.16 \pm 0.09	0.22 \pm 0.09	0.38 \pm 0.11
C:1	22.22 \pm 1.71	26.87 \pm 1.71 [*]	30.90 \pm 0.33 ^{*#}
C:2	77.73 \pm 1.70	72.98 \pm 1.70 [*]	68.72 \pm 0.24 ^{*#}

^a Values are mean \pm SD of three independent replicates. Significance level: ^{*,#} $p < 0.05$. ^{*} Significant difference of LH03 or LH09 compared with LH. [#] Significant difference of LH03 compared with LH09. nd, non detected.

TABLE S10. Composition, chain length and degree of unsaturation of PG molecular species found in the parental yeast strain LH and their corresponding myriocin-evolved clones LH03 and LH09.

PG specie	mol % of total PG \pm SD ^a		
	LH	LH09	LH03
C32:1	19.85 \pm 0.24	25.85 \pm 2.17 [*]	27.85 \pm 0.51 [*]
C32:2	8.69 \pm 0.88	7.31 \pm 0.40 [*]	7.46 \pm 1.40
C34:1	49.42 \pm 3.95	51.17 \pm 2.40	50.39 \pm 0.95
C34:2	22.04 \pm 2.84	15.67 \pm 0.43 [*]	14.30 \pm 0.44 ^{*#}
Total chain length			
C32	28.54 \pm 1.11	33.16 \pm 2.00 [*]	35.31 \pm 1.02 [*]
C34	71.46 \pm 1.11	66.84 \pm 2.00 [*]	64.69 \pm 1.02 [*]
Degree of unsaturation			
C:1	69.26 \pm 3.71	77.02 \pm 0.33 [*]	78.25 \pm 1.43 [*]
C:2	30.74 \pm 3.71	22.98 \pm 0.33 [*]	21.75 \pm 1.43 [*]

^a Values are mean \pm SD of three independent replicates. Significance level: ^{*,#} $p < 0.05$. ^{*} Significant difference of LH03 or LH09 compared with LH. [#] Significant difference of LH03 compared with LH09. nd, non detected.

TABLE S11. Composition, chain length and degree of unsaturation of PI molecular species found in the parental yeast strain LH and their corresponding myriocin-evolved clones LH03 and LH09.

PI specie	mol % of total PI \pm SD ^a		
	LH	LH09	LH03
C26:0	2.27 \pm 0.24	3.73 \pm 0.42 [*]	3.60 \pm 0.16 [*]
C26:1	0.98 \pm 0.57	1.37 \pm 0.80	1.06 \pm 0.62
C28:0	1.74 \pm 0.11	2.33 \pm 0.17 [*]	2.34 \pm 0.11 [*]
C28:1	0.80 \pm 0.08	0.81 \pm 0.04	0.71 \pm 0.09
C30:0	0.36 \pm 0.01	0.42 \pm 0.02 [*]	0.53 \pm 0.01 ^{*#}
C30:1	1.56 \pm 0.02	1.58 \pm 0.06	1.77 \pm 0.24
C30:2	0.24 \pm 0.02	0.18 \pm 0.01 [*]	0.18 \pm 0.04 [*]
C32:1	16.74 \pm 0.64	22.07 \pm 0.95 [*]	23.67 \pm 0.70 ^{*#}
C32:2	5.31 \pm 0.24	5.30 \pm 0.32	5.14 \pm 0.63
C34:1	43.12 \pm 1.54	43.36 \pm 1.41	44.27 \pm 1.85
C34:2	16.78 \pm 1.34	11.99 \pm 0.60 [*]	10.81 \pm 0.66 ^{*#}
C36:1	8.62 \pm 0.69	6.12 \pm 0.57 [*]	5.43 \pm 0.44 [*]
C36:2	2.15 \pm 0.19	1.20 \pm 0.17 [*]	0.85 \pm 0.03 ^{*#}
Total chain length			
C26	2.59 \pm 0.54	4.65 \pm 1.18 [*]	4.30 \pm 0.47 [*]
C28	2.54 \pm 0.15	3.14 \pm 0.21 [*]	3.05 \pm 0.18 [*]
C30	2.16 \pm 0.02	2.17 \pm 0.05 [*]	2.48 \pm 0.27 [*]
C32	22.04 \pm 0.41	27.36 \pm 1.26 [*]	28.81 \pm 1.33 [*]
C34	59.89 \pm 0.21	55.35 \pm 1.91 [*]	55.08 \pm 1.22 [*]
C36	10.77 \pm 0.86	7.32 \pm 0.73 [*]	6.28 \pm 0.41 ^{*#}
Degree of unsaturation			
C:0	4.37 \pm 0.35	6.48 \pm 0.58 [*]	6.47 \pm 0.26 [*]
C:1	71.16 \pm 1.43	74.85 \pm 0.63 [*]	76.56 \pm 1.51 [*]
C:2	24.46 \pm 1.78	18.66 \pm 0.52 [*]	16.98 \pm 1.35 [*]

^a Values are mean \pm SD of three independent replicates. Significance level: ^{*},[#] $p < 0.05$. ^{*} Significant difference of LH03 or LH09 compared with LH. [#] Significant difference of LH03 compared with LH09. nd, non detected.

TABLE S12. Composition, chain length and degree of unsaturation of PS molecular species found in the parental yeast strain LH and their corresponding myriocin-evolved clones LH03 and LH09.

PS specie	mol % of total PS \pm SD ^a		
	LH	LH09	LH03
C30:1	0.80 \pm 0.46	0.70 \pm 0.15	0.85 \pm 0.18
C32:1	12.52 \pm 0.62	16.66 \pm 0.63 [*]	17.57 \pm 0.70 [*]
C32:2	5.32 \pm 0.20	5.68 \pm 0.26	5.75 \pm 0.12 [*]
C34:1	42.36 \pm 1.14	45.71 \pm 0.72 [*]	47.63 \pm 0.91 ^{**}
C34:2	36.20 \pm 1.63	28.96 \pm 0.73 [*]	25.92 \pm 0.23 ^{**}
C36:1	1.24 \pm 0.08	1.20 \pm 0.13 [*]	1.36 \pm 0.02 [*]
C36:2	1.83 \pm 0.12	1.08 \pm 0.03 [*]	0.91 \pm 0.06 ^{**}
Total chain length			
C30	0.80 \pm 0.46	0.70 \pm 0.15	0.85 \pm 0.18
C32	17.84 \pm 0.42	22.35 \pm 0.87 [*]	23.31 \pm 0.81 [*]
C34	78.56 \pm 0.61	74.67 \pm 0.97 [*]	73.55 \pm 0.98 [*]
C36	3.07 \pm 0.19	2.29 \pm 0.12 [*]	2.28 \pm 0.07 [*]
Degree of unsaturation			
C:1	56.65 \pm 1.94	64.27 \pm 0.71 [*]	67.42 \pm 0.13 ^{**}
C:2	43.35 \pm 1.94	35.73 \pm 0.71 [*]	32.58 \pm 0.13 ^{**}

^a Values are mean \pm SD of three independent replicates. Significance level: ^{*},[#] $p < 0.05$. ^{*} Significant difference of LH03 or LH09 compared with LH. [#] Significant difference of LH03 compared with LH09. nd, non detected.

TABLE S13. Single point differences between parental (LH) and evolved strain LH03^a.

Chr.	Position	SNP frequency (%)			Affected Gene	Change	Effects ^b	
		LH	LH03	LH09			Variant type	Codon usage
II	168,941	2.9	20.0	0.0	<i>RPL19B</i>	GTC>GTT	syn (V>V)	0,21>0,39
II	168,950	4.4	21.4	4.3	<i>RPL19B</i>	GGA>GGT	syn (G>G)	0,12>0,47
II	168,959	2.9	16.7	4.5	<i>RPL19B</i>	GTC>GTA	syn (V>V)	0,21>0,21
II	169,058	2.5	17.1	4.6	<i>RPL19B</i>	ACT>ACC	syn (V>V)	0,35>0,22
II	169,067	2.2	15.6	4.1	<i>RPL19B</i>	GCT>GCC	syn (A>A)	0,38>0,22
II	170,308	0.0	19.1	0.0		A>G	n.a.	n.a.
II	170,310	0.0	16.3	0.0		A>C	n.a.	n.a.
II	320,417	2.8	22.9	6.6	<i>CST26</i>	TGA>TAA	syn (STOP>STOP)	0,29>0,48
IV	134,438	1.7	31.1	3.9	<i>LYS20</i>	ATC>ATT	syn (I>I)	0,26>0,46
IV	134,480	4.4	24.0	4.8	<i>LYS20</i>	GCC>GCA	syn (A>A)	0,22>0,29
IV	134,492	4.7	24.5	0.0	<i>LYS20</i>	CAG>CAA	syn (Q>Q)	0,31>0,69
IV	491,928	4.7	16.3	2.2	<i>RPS11A</i>	GTT>GTC	syn (V>V)	0,39>0,21
IV	492,018	4.0	23.8	3.1	<i>RPS11A</i>	GAC>GAT	syn (D>D)	0,35>0,65
IV	492,228	3.1	25.0	1.0	<i>RPS11A</i>	GTC>GTT	syn (V>V)	0,21>0,39
IV	492,231	4.1	21.6	1.0	<i>RPS11A</i>	GCC>GCT	syn (A>A)	0,22>0,38
IV	492,270	4.8	17.5	0.0	<i>RPS11A</i>	GTT>GTC	syn (V>V)	0,39>0,21
IV	492,291	4.0	16.7	0.0	<i>RPS11A</i>	GCT>GCC	syn (A>A)	0,38>0,22
IV	492,300	4.2	16.7	0.0	<i>RPS11A</i>	GCT>GCC	syn (A>A)	0,38>0,22
IV	492,306	4.3	16.7	0.0	<i>RPS11A</i>	AAA>AAG	syn (K>K)	0,58>0,42
IV	1,088,636	4.4	20.0	4.7	<i>SSF2</i>	TTA>TTG	syn (L>L)	0,28>0,29
IV	1,088,725	3.1	18.9	4.7	<i>SSF2</i>	AGA>AAA	miss (R>K)	0,48>0,58
IV	1,360,567	1.7	19.6	3.4	<i>RPS18A</i>	GTT>GTC	syn (V>V)	0,39>0,21
IV	1,360,573	1.8	17.4	4.3	<i>RPS18A</i>	AAT>ATC	syn (T>T)	0,46>0,26
IV	1,360,591	0.8	17.5	3.4	<i>RPS18A</i>	CAC>CAT	syn (H>H)	0,36>0,64
IV	1,360,597	1.7	23.8	2.8	<i>RPS18A</i>	AAA>AAG	syn (K>K)	0,58>0,42
IV	1,360,606	1.6	23.8	2.1	<i>RPS18A</i>	GCT>GCC	syn (A>A)	0,38>0,22
IV	1,360,615	1.7	25.0	2.3	<i>RPS18A</i>	TTG>TTA	syn (L>L)	0,29>0,28
IV	1,360,627	1.7	23.8	2.9	<i>RPS18A</i>	AAT>AAC	syn (N>N)	0,59>0,41
IV	1,360,633	1.7	26.2	3.0	<i>RPS18A</i>	ATC>ATT	syn (I>I)	0,26>0,46
IV	1,360,681	2.0	25.0	3.2	<i>RPS18A</i>	AAA>AAG	syn (K>K)	0,58>0,42
IV	1,360,711	1.9	22.5	3.6	<i>RPS18A</i>	AAA>AAG	syn (K>K)	0,58>0,42
IV	1,360,720	2.0	22.2	2.2	<i>RPS18A</i>	GCT>GCC	syn (A>A)	0,38>0,22
IV	1,360,723	1.9	19.4	3.0	<i>RPS18A</i>	CAT>CAC	syn (H>H)	0,64>0,36
IV	1,360,732	2.0	21.1	3.2	<i>RPS18A</i>	ATC>ATT	syn (I>I)	0,26>0,46
IV	1,360,750	2.2	19.1	3.6	<i>RPS18A</i>	TTG>TTA	syn (L>L)	0,29>0,28
V	326,002	0.0	17.5	2.0		AT>A	n.a.	n.a.
V	397,296	2.9	15.2	3.2	<i>RPL23B</i>	GTT>GTC	syn (V>V)	0,39>0,21
V	397,302	3.4	17.1	3.5	<i>RPL23B</i>	GCT>GCC	syn (A>A)	0,38>0,22
V	397,347	3.9	19.4	5.8	<i>RPL23B</i>	ATC>ATT	syn (I>I)	0,26>0,46
VI	194,604	0.0	29.5	2.5		TTA>T	n.a.	n.a.
VII	787,669	2.6	21.1	2.9	<i>RPL24B</i>	GCT>GCC	syn (A>A)	0,38>0,22
IX	177,481	0.0	21.2	0.0		A>G	n.a.	n.a.
IX	245,697	1.6	22.7	0.5		G>A	n.a.	n.a.
IX	317,839	0.0	23.5	7.0	<i>RPL2B</i>	ACT>ACC	syn (T>T)	0,35>0,22
IX	317,872	0.0	20.5	7.8	<i>RPL2B</i>	GCT>GCC	syn (A>A)	0,38>0,22
IX	317,884	0.0	20.5	7.8	<i>RPL2B</i>	GCT>GCC	syn (A>A)	0,38>0,22
IX	317,896	0.0	23.1	7.4	<i>RPL2B</i>	ACC>ACT	syn (T>T)	0,22>0,35
XI	68,106	3.6	20.4	2.3		A>AAAAAAT	n.a.	n.a.
XI	68,113	3.9	23.5	2.4		T>A	n.a.	n.a.

TABLE S13 (Continuation)

Chr.	Position	SNP frequency (%)			Affected Gene	Change	Effects ^b	
		LH	LH03	LH09			Variant type	Codon usage
XI	68,117	4.3	27.1	2.7		G>A	n.a	n.a.
XI	235,973	0.0	33.3	4.7		G>GTA	n.a	n.a.
XII	139,773	2.2	29.0	6.2	<i>SPO75</i>	TGC>TGT	syn (C>C)	0,37>0,63
XII	460,686	3.9	25.1	1.4		A>A ₆ GA ₄ T	n.a	n.a.
XII	460,720	0.0	16.2	1.4		T>A	n.a	n.a.
XII	460,722	4.9	21.3	4.1		GTA>G:	n.a	n.a.
XIII	8,370	4.8	28.1	2.6	<i>COS3</i>	GTG>GAG	miss (V>E)	0,19>0,29
XIII	8,373	4.8	23.3	2.5	<i>COS3</i>	CTC>CCC	miss (L>P)	0,06>0,15
XIII	37,749	0.0	17.7	3.6	<i>YML116W-A</i>	T>0	frameshift	n.a.
XIII	550,539	4.8	20.5	3.0	<i>RPL13B</i>	TAC>TAT	syn (Y>Y)	0,44>0,56
XIII	550,674	2.9	17.5	1.7	<i>RPL13B</i>	GCC>GCT	syn (A>A)	0,22>0,38
XIV	181,308	4.6	17.1	3.9		C>CA	n.a	n.a.
XIV	258,275	0.0	21.9	0.0		G>A	n.a	n.a.
XIV	500,112	4.4	21.2	1.4	<i>RPL9B</i>	ATC>ATT	syn (I>I)	0,26>0,46
XIV	500,118	4.3	20.8	1.4	<i>RPL9B</i>	TTA>TTG	syn (L>L)	0,28>0,29
XIV	500,121	4.4	21.2	1.4	<i>RPL9B</i>	TCT>TCA	syn (S>S)	0,26>0,21
XIV	500,133	3.4	23.4	0.9	<i>RPL9B</i>	GTT>GTC	syn (V>V)	0,39>0,21
XIV	500,151	2.1	27.7	0.9	<i>RPL9B</i>	AAT>AAC	syn (N>N)	0,59>0,41
XIV	500,154	2.0	29.8	0.9	<i>RPL9B</i>	GCC>GCT	syn (A>A)	0,22>0,38
XIV	500,181	1.5	24.4	0.0	<i>RPL9B</i>	GTT>GTC	syn (V>V)	0,39>0,21
XIV	500,202	1.6	25.0	0.0	<i>RPL9B</i>	AAG>AAA	syn (K>K)	0,42>0,58
XIV	561,332	0.0	22.6	3.6		G>A	n.a	n.a.
XV	235,401	0.0	18.6	0.0	<i>GAL11</i>	CAG>CAA	syn (Q>Q)	0,31>0,69
XV	235,404	0.0	19.0	0.0	<i>GAL11</i>	CAG>CAA	syn (Q>Q)	0,31>0,69
XV	235,407	0.0	18.6	0.0	<i>GAL11</i>	CAG>CAA	syn (Q>Q)	0,31>0,69
XV	326,506	0.0	40.6	0.0		T>A	n.a	n.a.
XV	692,618	0.0	26.2	0.0	<i>ULS1</i>	GTC>GTT	syn (V>V)	0,21>0,39
XVI	436,481	4.9	38.3	3.5		A>G	n.a	n.a.
XVI	747,862	2.3	19.6	2.7	<i>DBF20</i>	CA>C	frameshift	n.a.

^a SNPs supported by >15% of the base calls for the position in the evolved strain and <5% of the calls in the parental strain. ^b syn, synonymous variant; miss, missense variant; n.a., non applicable.

TABLE S14. Single point differences between parental (LH) and evolved strain LH09^a.

Chr.	Position	SNP frequency (%)			Affected Gene	Change	Effects ^b	
		LH	LH03	LH09			Variant type	Codon usage
IV	383449	4.7	11.8	15.6	<i>PRM7</i>	GAC>GAT	syn (D>D)	0,35>0,65
V	455615	0.0	0.0	27.0	<i>MAG1</i>	AGT>ATT	miss (S>I)	0,16>0,46
VI	268205	0.0	5.9	23.5		A>AAT	n.a.	n.a.
VIII	146752	0.0	0.1	15.7		G>A	n.a.	n.a.
XI	146918	4.3	6.7	26.1		C>T	n.a.	n.a.
XIII	721996	0.0	0.0	29.6	<i>YMR226C</i>	ATC>ACC	miss (I>T)	0,26>0,22
XV	92645	0.0	0.0	41.7		AT>A	n.a.	n.a.
XV	108996	0.8	1.7	45.4		T>C	n.a.	n.a.
XV	108997	0.8	1.7	46.6		CT>C	n.a.	n.a.
XV	849793	0.0	0.0	20.8	<i>RDL1</i>	TCG>TCC	syn (S>S)	0,1>0,16

^a SNPs supported by >15% of the base calls for the position in the evolved strain and <5% of the calls in the parental strain. ^b syn, synonymous variant; miss, missense variant; n.a., non applicable.

TABLE S15. Single point differences with the parental strain (LH) common in both evolved strains (LH03 and LH09)^a.

Chr.	Position	SNP frequency (%)			Affected Gene	Change	Effects ^b		
		LH	LH03	LH09			Variant type	Codon usage	
II	320502	4.5	18.6	21.7	<i>CST26</i>	ATT>GAT	miss (N>D)	0,59>0,65	
II	586459	0.0	29.3	21.8		G>GA	n.a	n.a	
II	586488	0.0	19.5	17.7		A>T	n.a	n.a	
III	273011	2.6	25.7	39.6		G>A	n.a	n.a	
III	63401	0.0	35.6	16.0		CG> C	n.a	n.a	
III	63403	0.0	35.1	16.2		A>C	n.a	n.a	
IV	501227	0.0	36.6	42.9	<i>YDR029W</i>	CGT>CAT	miss (R>H)	0,15>0,64	
V	156147	0.0	43.2	25.6		TC>T	n.a	n.a	
V	373393	0.0	29.2	57.7		T>TA	n.a	n.a	
V	156159	2.7	44.4	26.3		T>C	n.a	n.a	
V	156151	0.0	42.5	26.3		G>A	n.a	n.a	
V	565610	4.4	25.8	19.7		G>A	n.a	n.a	
V	565623	3.9	23.0	18.0		C>T	n.a	n.a	
VII	483370	4.1	16.7	27.6		<i>BRP1</i>	TTA>TTG	syn (L>L)	0,28>0,29
VII	508794	3.0	32.8	24.4			G>GTCT ₄ ATCT ₄ A	n.a	n.a
VIII	365433	0.0	33.3	16.7	<i>YHR131C</i>	GAT>GAC	syn (D>D)	0,65>0,35	
X	228720	4.8	32.6	31.2		T>C	n.a	n.a	
XI	13740	1.5	58.2	46.9		TC>T	n.a	n.a	
XII	937372	4.0	20.9	15.1		TA>T	n.a	n.a	
XII	208656	2.8	26.8	19.3		T>TAAGA	n.a	n.a	
XII	225364	0.9	49.4	20.3		T>TA	n.a	n.a	
XIII	158979	2.9	17.4	16.1		C>CT	n.a	n.a	
XIII	855378	3.6	30.0	61.2		A>AT	n.a	n.a	
XIV	308657	0.0	66.7	68.1		G>C	n.a	n.a	
XIV	308655	0.0	67.8	69.3		CT>C	n.a	n.a	
XIV	628629	1.8	40.5	51.1		A>AC	n.a	n.a	
XV	436844	0.0	23.3	26.1		T>TA	n.a	n.a	

^a SNPs supported by >15% of the base calls for the position in the evolved strain and <5% of the calls in the parental strain. ^b syn, synonymous variant; miss, missense variant; n.a., non applicable.